

zapomniane



**Report on Research at the Jewish Cemetery
in Działoszyce
aimed at determining the location of a mass grave
from the time of the Holocaust**

Authors: Dr. Sebastian Różycki; Dr. Szymon Oryński; Aleksander Schwarz

Contents

Overview of the research process.....	3
History of the area.....	3
Execution Sites and Locations of Mass Graves.....	5
Analysis and Interpretation of Historical Aerial Photographs.....	7
1939-1945 aerial photographs available in the United States National Archives and Record Administration (NARA), Record Group 373.....	8
The obtained photographs.....	9
Technical description of the obtained photograph.....	9
Aerial photographs, orthophotomaps, and laser scanning data from the National Geodetic and Cartographic Resources.....	10
Research methodology.....	11
Cemetery fence.....	12
Geodetic research.....	19
Summary of the geodetic research.....	23
Geophysical research.....	24
Methodology.....	24
Results of the geophysical research.....	28
Summary of results of the geophysical research.....	44
Conclusions.....	45

Overview of the research process

This report summarizes the research conducted by the Zapomniane Foundation and its experts between February and May 2025. The research was carried out in accordance with the principles of Jewish religious law (Halacha) and the guidelines of the Rabbinical Commission for Jewish Cemeteries in Poland. The research process included:

- Analysis and interpretation of historical aerial photographs to determine the research area,
- Geodetic research: marking the research area and preparing a map for non-invasive studies,
- Geophysical research: research using ground-penetrating radar (GPR),
- Geophysical research: research using magnetometry,
- Geophysical research: research using conductivity measurements.

History of the area

The research was conducted in the town of Działoszyce, located in the southern part of the Świętokrzyskie Voivodeship, in Pińczów County. The town is situated at the confluence of the Jakubówka and Sancygniówka rivers, the latter being a tributary of the Nidzica River. This area is characterized by a long and well-documented history of settlement, dating back at least to the 13th century, as evidenced by the earliest written sources. As a result of the Third Partition of Poland in 1795, Działoszyce came under the control of the Habsburg monarchy, remaining in Austrian partition for twelve years. From 1807 to 1815, the town was part of the Duchy of Warsaw, and in 1815 – following the decisions of the Congress of Vienna – it was incorporated into the Russian Empire, where it remained for over a hundred years. The town's proximity to the Austrian border and its location near the Free City of Kraków fostered settlement development, including a significant increase in Jewish settlement, particularly in the 19th century. During the Second Polish Republic, Działoszyce served as a local center for agricultural trade (mainly grain, poultry, and livestock) and was home to several small industrial workshops. According to the 1921

census, the town had 6,755 residents, about 80% of whom were Jewish. By 1939, the population had decreased to 5,872. During the German occupation, the Jewish community was subjected to extermination. After the annexation of Upper Silesia by the Third Reich, many Jews and Poles fled toward the General Government, leading to an increase in the population of the Działoszyce region. On September 2, 1942, Gestapo units from Miechów arrived in the town and issued an order for the entire Jewish population – both from Działoszyce and nearby villages – to assemble in the town square. By the end of the day, approximately 10,000 people had gathered there. On September 3, an order was given to transport those assembled to a collection point near Miechów and then – primarily – to the extermination camp in Bełżec. Most were sent on foot to the railway station. Approximately 1,500 individuals, including the elderly and those unable to walk, were loaded onto horse-drawn carts and trucks and taken to the Jewish cemetery, where they were executed. Their bodies were buried in three mass graves. In the days that followed, German soldiers searched the homes abandoned by the Jewish population, confiscating and removing movable property. Deportations and mass killings led to the near-total destruction of the Jewish community in Działoszyce and a significant decline in population – by the end of the war, the town had fewer than 2,000 inhabitants.

The near-surface geological structure in the Działoszyce region is dominated by Pleistocene aeolian formations, primarily loess and dust deposits. These layers generally range in thickness from several to over a dozen meters and exhibit significant morphological variability both regionally and locally. Complementing the geological profile are the flat-bottomed valleys of the Jakubówka, Sancygniówka, and Nidzica rivers, whose deposits consist of Holocene river sands and silts that fill floodplain terraces and valley floors. These deposits are adjacent to glacial tills associated with the glacial complexes of southern Poland. Locally, the subsoil may contain outcrops of Miocene-age gypsum or anhydrite, often found in association with interbedded clays, marls, marly limestones, as well as rock salt and limestones containing sulfur – all of which are lithostratigraphic units belonging to the Krzyżanowice Formation. In summary, the area covered by the geophysical surveys is characterized by a dominance of loess and dust deposits with low electrical resistivity, locally interspersed with glacial till layers and alluvial sediments.

Execution Sites and Locations of Mass Graves

On the evening of 2 September, a liquidation group arrived in Działoszyce by narrow-gauge railway. According to Chaim Icchak Wolgelernter, it was 200 Germans and 300 Baudienst jawans. Another account mentions the participation of several Gestapo men, as well as gendarmes and blue policemen. The mayor of the town was ordered to post notices informing the Jews of the place of the forced assembly, and forbidding the Polish population to help Jews under penalty of death (Figure 1).

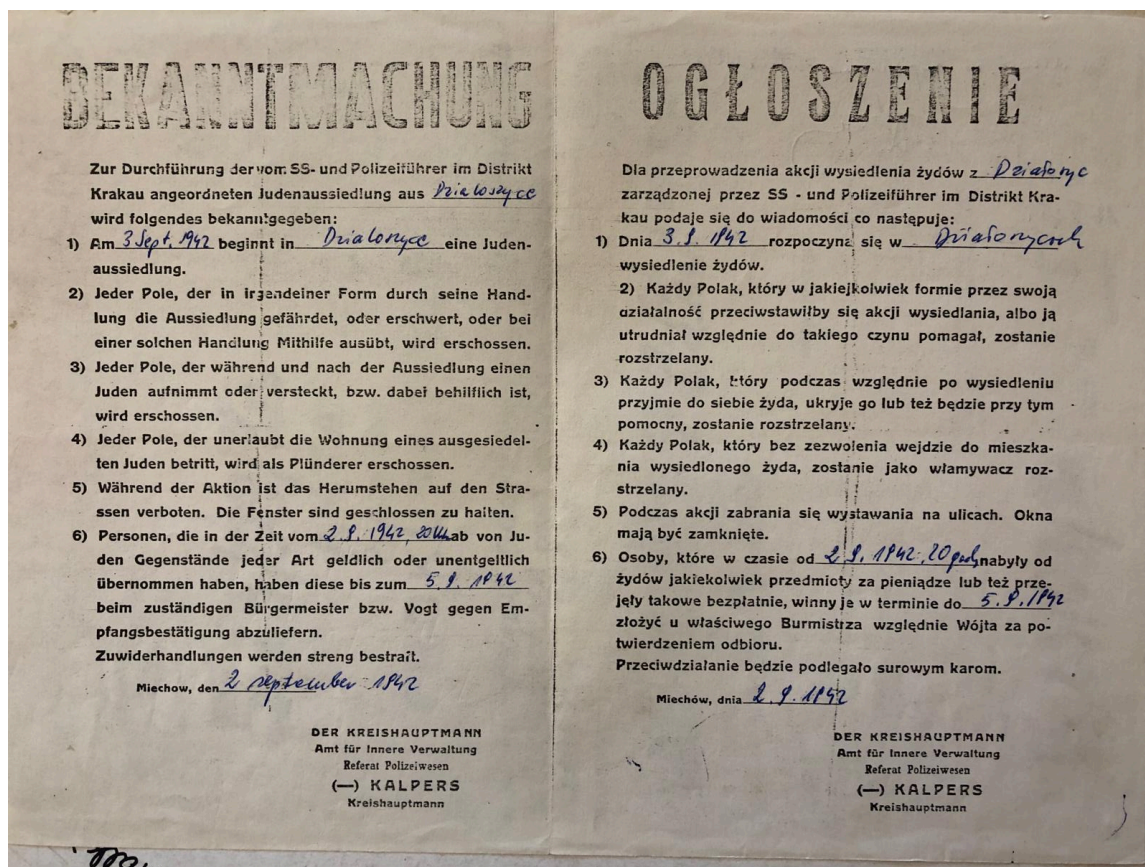


Figure 1. A notice informing Jews of the place of the forced assembly and forbidding the Polish population to help Jews under penalty of death.

The next morning the manhunt began. Jewish residents of the town were driven out of their homes, caught in the streets and rounded up in the market square. Many people were shot, including Rabbi Mordka Ick Staszewski. People began to be taken to the Jewish cemetery, where three large pits were dug during the night by the Junkers. By 2pm the gendarmes and Gestapo men had murdered between 1,200 and 1,500 people. Beyerlein, Riedinger and Karl from Miechow were present, as well as

probably officers from the 65th Police Battalion stationed in Krakow. Before being killed, the victims were ordered to undress and line up over a ditch. They were then shot in the occiput. After the execution, the pits were buried by the jawans. Those murdered during the actions in the streets of Działoszyce were also buried there.

A field inspection was carried out on 14 November 1968, at which witnesses pointed out the place of execution. During the field inspection, several photographs were taken showing the place indicated and found (Figure 2 and 3).



Figure 2. The road leading to the execution site (IPN).



Figure 3. Escarpment, where executions took place in 1942 (IPN).

Thanks to the efforts of the Municipal Council Działoszyce, part of the former cemetery site was demarcated in 1989 and a memorial was erected to the Jewish inhabitants who were murdered by the occupying forces in 1942. Using the visible escarpment and single trees, it is possible to locate where the photographs were taken and, at the same time, where the executions took place.

Analysis and Interpretation of Historical Aerial Photographs

In order to interpret the area of the Jewish cemetery in Działoszyce, archival search queries were carried out to find and obtain photogrammetrical and cartographic materials. The US Archives and the Head Office of Geodesy and Cartography (Główny Urząd Geodezji i Kartografii, GUGiK) in Poland were searched. Other material (testimonies and ground photographs) was also obtained and used in the search for execution sites and the location of mass graves.

1939-1945 aerial photographs available in the United States National Archives and Record Administration (NARA), Record Group 373

As part of an order to search for aerial photographs, search queries were performed in the United States National Archives and Records Administration¹ (NARA) for photographs covering the cemetery area in Działoszyce from 1939 to 1945. The search query concerned group 373 collections.

The collections in group 373 comprise sets of aerial and satellite photographs, as well as cartographic and architectural materials. The search query included 373.3 series consisting of aerial photographs taken in 1935 to 1960 by both German and Allied airmen².

The photographs available in the archives are shared on a public domain basis.

Information from the website of the United States National Archives on public domain, possibility of using and indicating the source:

“The vast majority of the digital images in the Online Catalog are in the public domain. Therefore, no written permission is required to use them. We would appreciate your crediting the National Archives and Records Administration as the original source.”

Based on the results of the search query conducted in the archives, a list of photographs was created for the cemetery and the photographs available were ordered in the archives.

¹ The Archives Address: National Archives at College Park, 8601 Adelphi Road, College Park, MD 20740-6001

² the collection of photographs taken by the Allied airmen consists of 2,863,800 pieces, and by the German airmen — 1,209,520

The obtained photographs

As part of the order, one German (Luftwaffe) aerial photographs were obtained and scanned with EPSON Expression 12000 XL scanner at 600 DPI. The original paper prints available in the archive were scanned. This is the only photo available in the archive for the cemetery area.

Technical description of the obtained photograph

1. **Signature: GX 12334**

A series of photographs taken with 200 mm cone Carl Zeiss RB-30 camera. The exact date the series of photographs: January 17, 1945. The obtained images are of poor quality (figure 4). The photo was taken at 11.09.



Figure 4. An aerial photograph taken in 1945.

Aerial photographs, orthophotomaps, and laser scanning data from the National Geodetic and Cartographic Resources

An orthophotograph is a product obtained by the geometric processing of an aerial photograph. This process, known as ortorectification, is commonly known as the change of the central projection to the orthogonal projection. An orthophoto is shown in a specific mapping and coordinate system and provides adequate situational accuracy. Unlike an orthophotomap, it does not maintain a prescribed section/sheet breakdown and does not become an end product, but is an intermediate product. An orthophotomap is a collection of mosaicked orthophotographs. In Poland, orthophotomaps collected in the Central Geodetic and Cartographic Resources are made available by the Head Office of Geodesy and Cartography. As part of the performed task, aerial photographs and orthophotomaps from **1957** (Figure 5), **1997**, and **2022** were collected for the cemetery. The selection of photographs was preceded by an analysis of the possible use of available photogrammetrical materials in Polish archives.

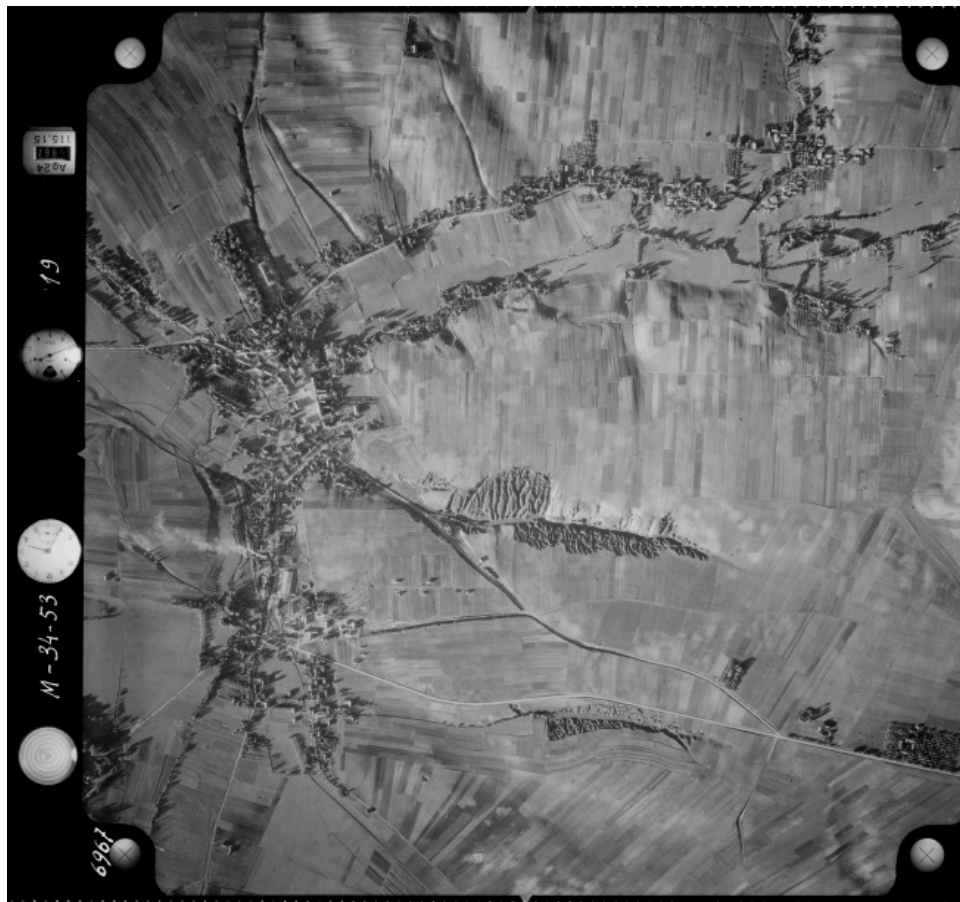


Figure 5. Aerial photograph from 1957 for the town of Działoszyce.

The archive materials described in this chapter in the form of aerial photographs allow the interpretation and analysis of the cemetery area. As part of the order being performed, the current spatial data set, available for the development area, was also acquired and described. This material will help refer the results of analyses and interpretations of archival materials to the current terrain situation. **This is of great importance for planning field studies, both non-invasive and invasive ones, as well as for future memorialising.**

Research methodology

To define the boundaries of the cemetery and for the sake of interpretation, archival and current data relating to the surrounding area will be used. Archival data in the form of aerial photographs taken **in 1957** are the main material for recreating the boundaries of the cemetery and for analysing the historical coverage of the area.

Current data in the form of aerial photographs will be used to reference (georeference) archival data and will allow visualization of the selected archival objects on the current background.

QGIS software was used for practical interpretation and analysis of the terrain. In the first stage of the works, vector layers were acquired, showing the cemetery border and the terrain objects seen in 1957 photograph: probable border, and Individual matzevot. The vector layers created allowed the creation of graphic attachments. All the data obtained from the interpretation have been written to the National Spatial Reference System: system 2000, zone 7 (UTM 34N for survey). This helped generate geodetic coordinates of the selected objects. These coordinates will allow to map the identified objects in the area in the aerial photographs taken in 1945 and 1957.

Cemetery fence

The initial location of the cemetery on the topographical map allowed the exact location of the object in the aerial photographs. In order to determine the border of the cemetery, data from the Land and Property Register was also used. The Land and Property Register, or the real estate cadastre, is a public register of spatial data on land, buildings, and premises, as well as data on property owners. The current **course of the land boundaries does not coincide with the boundaries of the cemetery** as seen in the 1957 photograph (Figure 6). The cemetery's border interpretation was also facilitated (only the southern boundary) by the form of an earth embankment of the cemetery, which survived in 1957. The wall is visible as a light line and a dark (almost black) shadow. If the wall was perpendicular to the light source, the shadow is visible as dark tones blocking objects on the other side of the earth embankment (not illuminated by the light source).



Figure 6. Orthophoto from 1957 with Land and Property Register (blue lines).

The rest course of the boundary was established on the basis of the texture filling the area, suspected to be that of a cemetery (Figure 7). The cemetery texture present, can be described as:

- grainy and irregular - resulting from the arrangement of gravestones and the vegetation between them,
- spotty and grainy - varied in terms of shadows and light reflections from the gravestones.



Figure 7. Orthophoto from 1957 with Land and Property Register (blue lines), and approximate boundary line (red lines).

The determined boundary allows **the area of the cemetery** from 1957 to be calculated — 12.800 m² (**1.28 ha**).

Individual large matzevot (in the form of monuments) are also visible in the cemetery area, casting a shadow in the 1957 photograph (Figure 8).



Figure 8. Orthophoto from 1957, blue lines are the current boundaries of the land cadastre, approximate boundary line (red lines), and Individual matzevot.

Using the texture described above, two additional areas adjacent to the cemetery were also delineated (Figure 9). These may be parts of the cemetery that have been used in recent times. However, these are not visible individual gravestones. The area to the north is bordered by arable fields and its texture may correspond to crops, such as potatoes. The designated additional areas could be subjected to a field visit and, in the future, to a detailed survey.



Figure 9. Ortophotomap from 1957. The blue lines are the current boundaries of the land cadastre. The cemetery border was marked in red. Areas that can be assigned as cemetery land (last period of operation) are outlined in black.

From testimonies we know that in the first days of September 1942 the Germans shot about 1500-1600 Jews, mostly elderly people, in the cemetery (according to other sources near the cemetery). The bodies were buried in the cemetery in mass graves.




The best material for delimiting such areas are aerial photographs from the Second World War. Unfortunately, the only available photo for the cemetery was taken in January 1945. The quality of the photo is very poor and does not allow to indicate the place of execution. In addition, the interpretation process is obstructed by snow lying on the ground.


The 1957 photograph does not show any ground disturbances that might indicate traces of mass graves. The cemetery area is evenly covered with low vegetation - including grass.

Based on the analysis, the markings visible on the maps below were prepared as a foundation for the subsequent stages of the research.

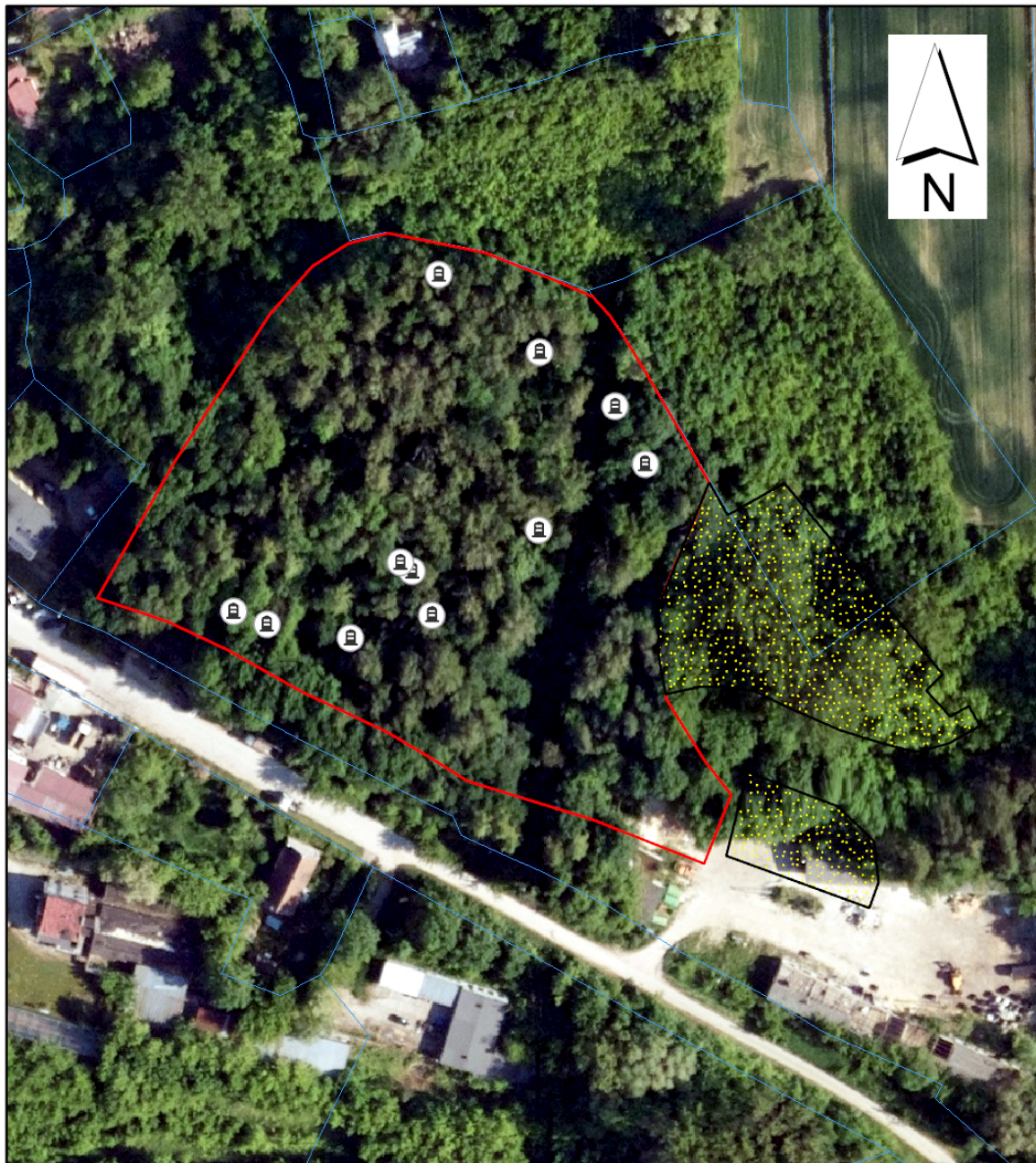


Legend




-  Individual matzevot
-  Possible boundary
-  Boundary

25 12,5 0 25 50 75 100
 Meters

Ortophoto from 1997. The blue lines are the current boundaries of the land cadastre. The cemetery border was marked in red. Areas that can be assigned as cemetery land (last period of operation) are outlined in black.



Legend

-  Individual matzevot
-  Possible boundary
-  Boundary

25 12,5 0 25 50 75 100
Meters

Ortophoto from 2022. The blue lines are the current boundaries of the land cadastre. The cemetery border was marked in red. Areas that can be assigned as cemetery land (last period of operation) are outlined in black.

Geodetic research

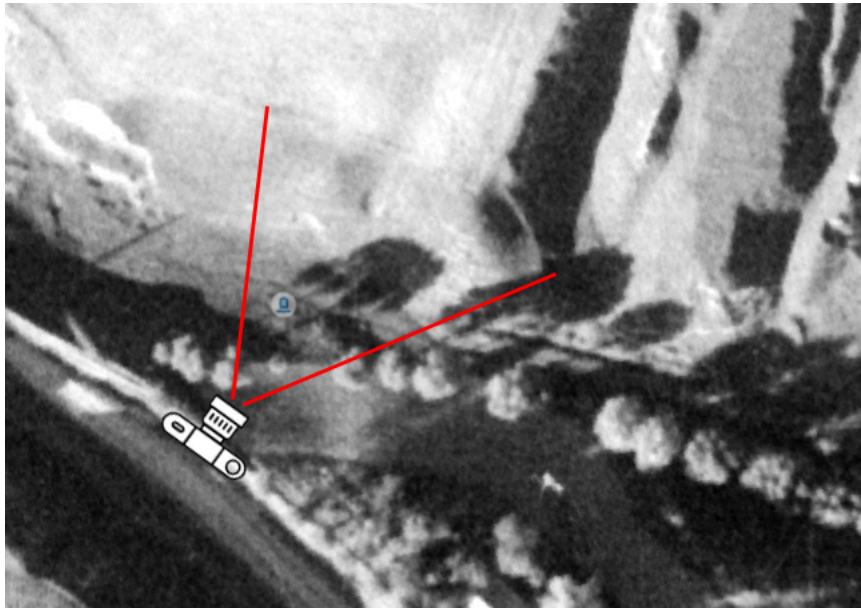


Figure 10. Ortophotomap from 1957. The site where the field inspection photo (on figure 8) was taken.

Research into the search for execution sites and mass graves in the close vicinity of the Jewish cemetery in Działoszyce was carried out in a methodical and multi-stage manner, with the aim of accurately selecting areas requiring further analysis. The process began with a field visit, which allowed direct study of the area and an assessment of its condition. A key element of this was a meeting with a person with knowledge provided by eyewitnesses to historical events. This person identified both the likely execution site and the location of the mass graves, which provided an important starting point for further work (Figure 11).





Figure 11. Photos from the field visit.

During the visit, the exact geographical coordinates of the identified sites were obtained, allowing them to be accurately marked on maps and in documentation. A series of photographs were also taken, which provide visual confirmation of the current state of the site and can serve as comparison material in the future (Figure 11). In addition, the site was scanned using a handheld LIDAR scanner. This technology allowed a detailed representation of the surface topography to be obtained, including the detection of small irregularities and terrain depressions. The latter, according to witness accounts, may correspond to execution sites and mass burials, making them priority points for further research.

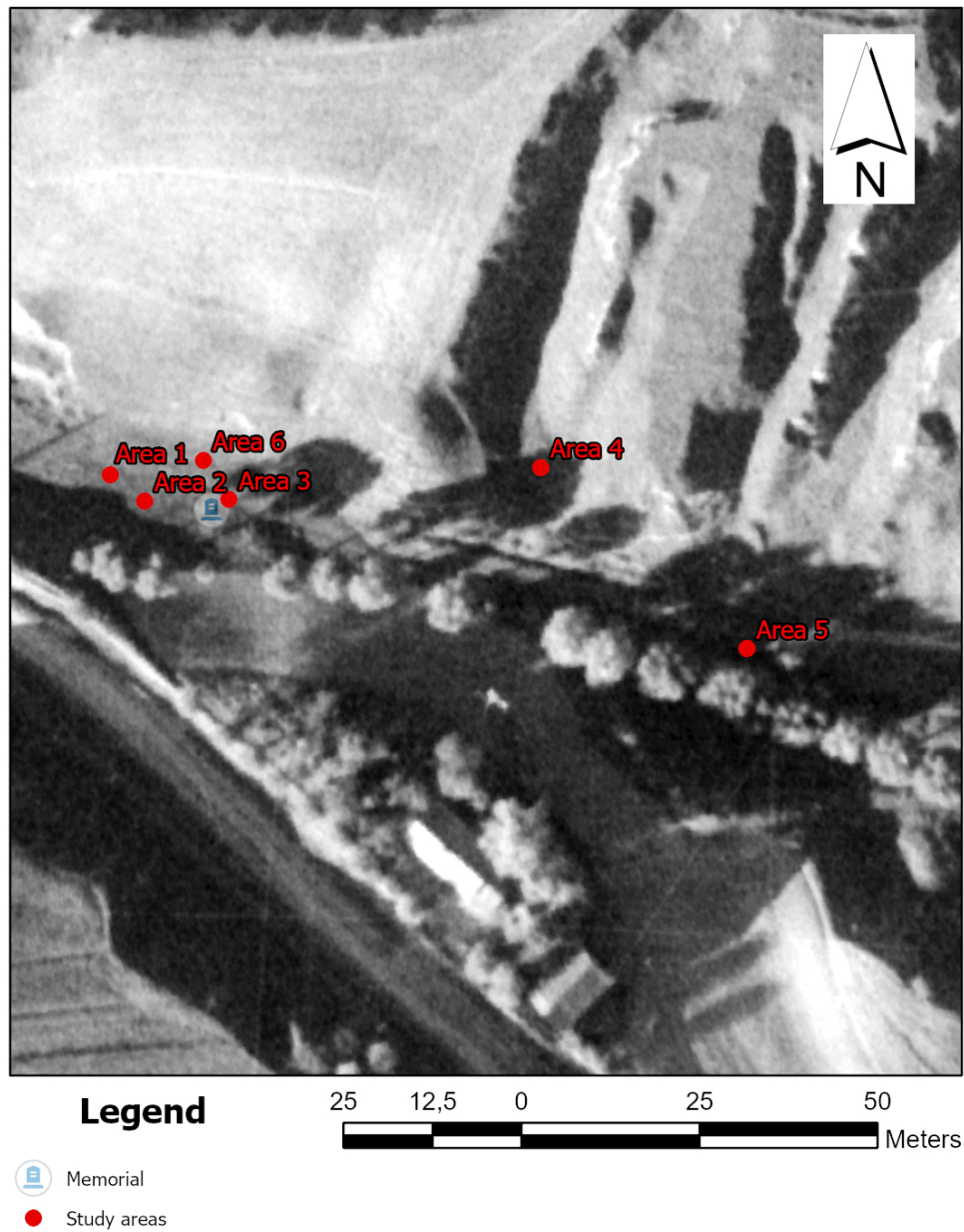


Figure 12. Ortophotomap from 1957. Locations of field-designated study areas

The data collected - coordinates, photographs and the results of the LIDAR scans - have formed a solid basis for planning the next stages of the work (Figure 13, 14, and 15).

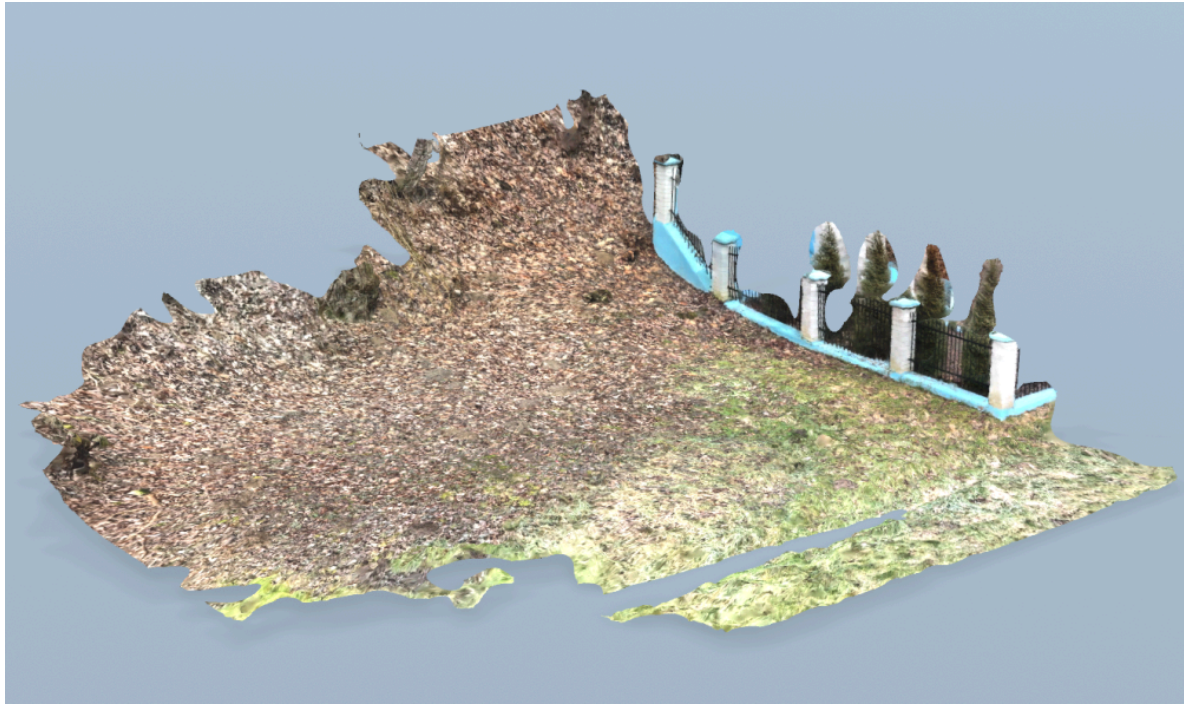


Figure 13. Terrain visualisation derived from laser scanning – area 2.

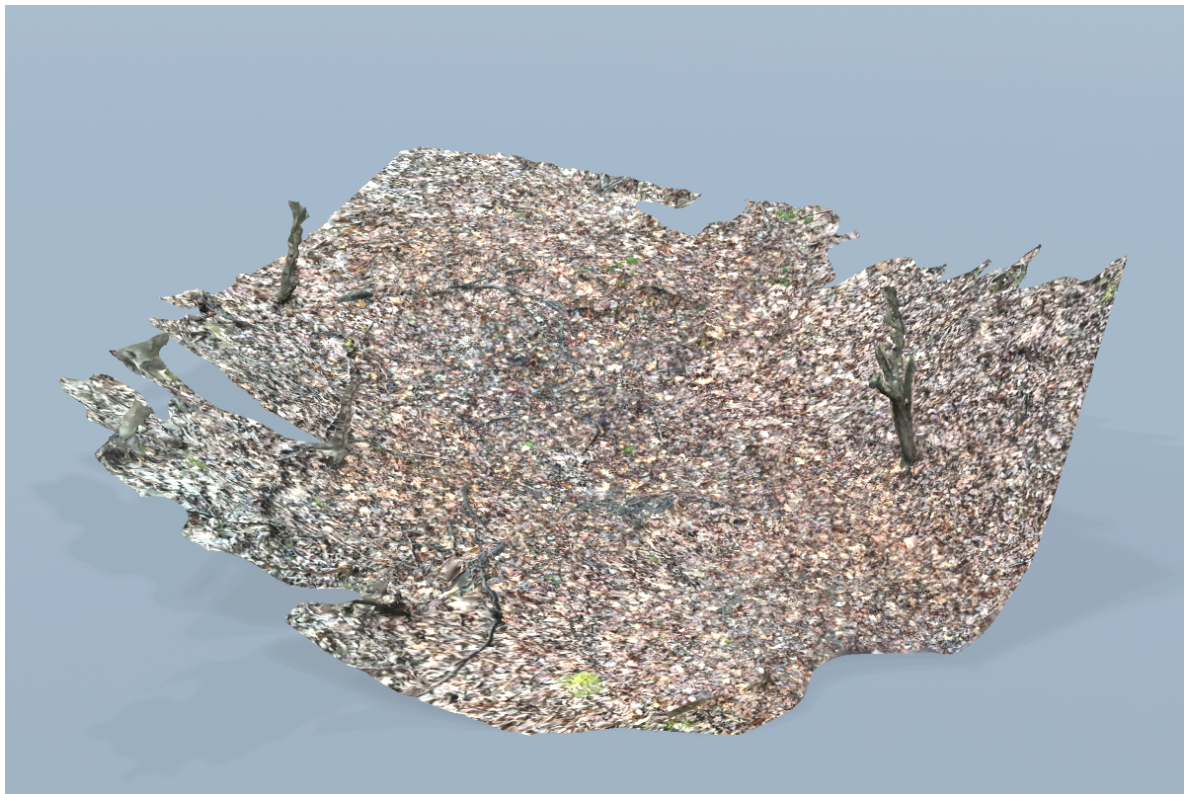


Figure 14. Terrain visualisation derived from laser scanning – area 4.

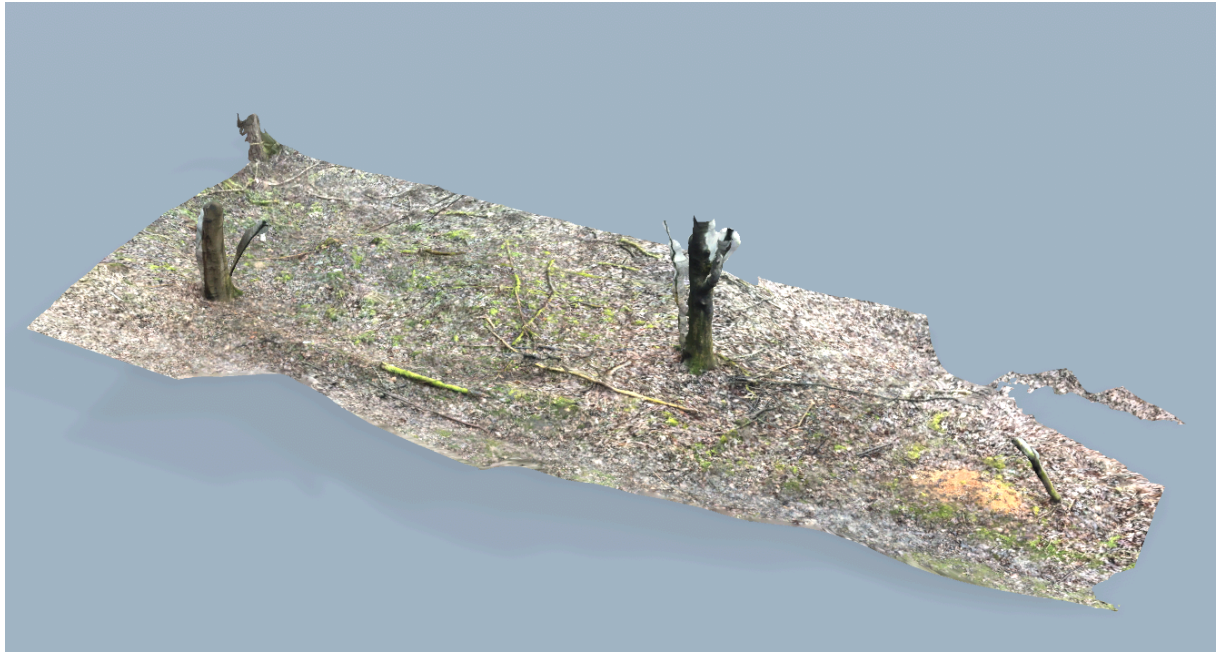


Figure 15. Terrain visualisation derived from laser scanning – area 5.

In the next phase, the identified areas are to be subjected to geophysical surveys, such as GPR or magnetometry, which will allow non-invasive examination of the ground structure and confirmation of the presence of anomalies that may indicate mass graves. This approach combines traditional methods based on witness accounts with modern technologies, increasing the chance of accurately locating and documenting sites of historical significance. Further analysis will be key to confirming the initial findings and preserving the memory of the tragic events associated with the site.

Summary of the geodetic research

The analysis of aerial photographs from 1944 and 1957, laser scanning data and the results of the field visit allowed the area to be selected for future geophysical surveys. The combination of historical archival material with modern technology and witness accounts has enabled the initial identification of sites requiring further confirmation, an important step in the process of documenting the area's past.

Geophysical research

Methodology

This chapter presents the characteristics of two geophysical methods that have found widespread application in archaeological research – gradient magnetometry and electromagnetic conductivity (EM) surveying. Both techniques belong to the group of non-invasive geophysical prospection methods and enable the identification of subsurface structures with varying physical properties, without the need for intrusive excavation. Their complementary nature allows for the effective detection of both anomalies related to anthropogenic modifications of the soil environment and natural lithological variations. The following sections of the chapter discuss the physical principles underlying each method, their range of applications, procedures for data acquisition, and the specific aspects of data interpretation in the context of archaeological investigations.

Magnetometry method

Magnetometry is a non-invasive, surface-based geophysical method that measures the intensity of the Earth's magnetic field. Variations in this field make it possible to detect different magnetic properties of the subsurface, which has led to applications across various disciplines. In geology, it is used to identify magmatic structures, while in engineering it is applied in the investigation of pipelines and the detection of unexploded ordnance. In archaeology, magnetometry enables the mapping of buried structures, hearths, and even graves.

Objects located within a magnetic field are subject to the phenomenon of induction, meaning they become magnetized. The degree of magnetization depends on the intensity vector T and the magnetic susceptibility of the material, which allows for the classification of substances into different categories. Diamagnetic, paramagnetic, and antiferromagnetic materials all exhibit different levels of magnetization. However, ferromagnetic materials interact most strongly with the magnetic field, causing measurable disturbances in its intensity. These anomalies are precisely what magnetometric prospection seeks to detect. Using this method, it is possible to infer the presence of various ferromagnetic structures and objects within the Earth's crust. The discovery of such anomalies may indicate the presence of ore deposits, crystalline

mineral bodies, magmatic veins, or archaeological and historical relics. Magnetometry is also useful in detecting components of underground infrastructure and utility networks.

In this study, a specific variant of the magnetometric method was applied—measurement of the vertical magnetic gradient. This technique involves the simultaneous measurement of the magnetic field using two sensors placed at different vertical positions. The greater the distance between the sensors, the deeper the investigation range of the method, allowing for detection at greater depths. The primary application area of this technique is archaeological research. It is a dedicated tool that enables the efficient identification of buried structures and hearths without the need for simultaneous reference measurements. As a result, the survey process is simplified, and the obtained data are both accurate and precise.

Electromagnetic conductivity method (FDEM)

The electromagnetic conductivity method (*FDEM* or *slingram*) is one of the electromagnetic techniques used in geophysical surveys. The functioning of a conductivity meter relies fundamentally on the generation, transmission, and reception of electric current. The instrument utilizes two coils, spaced at a distance s from each other. The first of these, the transmitter coil, generates a low-frequency alternating current (typically in the range of several to several tens of kilohertz). When current flows through the transmitter coil, it produces a time-varying magnetic field, referred to as the primary magnetic field (H_p). This primary field plays a key role, as it penetrates the subsurface medium. As a result, eddy currents are induced in the ground, giving rise to a secondary magnetic field.

The receiver coil, placed at a fixed distance from the transmitter, registers this secondary magnetic field generated in the subsurface. This process operates according to the principle of magnetic induction, which induces a voltage (and thereby a current) in the receiver. There is a direct correlation between the electrical conductivity of the subsurface (as affected by magnetic induction) and the difference in magnetic field strength between the primary field generated by the transmitter coil (H_p) and the secondary field measured by the receiver coil (H_s).

In the present study, a conductivity meter equipped with six transmitter–receiver coil pairs was used, allowing for simultaneous measurements of ground conductivity at six different investigation depths. Two key parameters are recorded during the survey: the apparent conductivity, which reflects variations in the electrical properties of the ground, and the relative amplitude of the vertical component of the magnetic field. This second parameter - known as the *in-phase* response - enables the detection of subsurface metallic objects.

Processing

Both methods require initial processing of the recorded measurement data, followed by proper interpretation in both geophysical and archaeological contexts. A detailed description of the individual stages of data processing will be presented separately for each of the discussed methods. Measurements using both techniques were carried out at five survey sites located in close proximity to one another. However, each of these areas represented a distinct interpretative challenge.

Three of the survey polygons were situated in the immediate vicinity of the Jewish Cemetery memorial in Działoszyce, while two additional survey areas were located at some distance, on opposite sides of a forest road. The survey terrain was characterized by a high degree of complexity in terms of its suitability for the applied geophysical methods. For the first three polygons, a major source of interference was the nearby power line. Additionally, metal fencing surrounding the memorial - located in close proximity to polygons 2 and 3 - had a significant impact on data quality. These areas exhibited the highest level of signal disturbance for both measurement methods.

The fourth polygon was located within a loess ravine on one side of the road, whereas the fifth was situated in a small depression on the opposite side. At these two sites, the main sources of interference were scattered metal debris such as wires, cans, old utensils, and bottle caps. Where possible, the area was cleared of surface debris prior to the commencement of measurements.

Magnetometry

The survey was conducted using a quasi-regular measurement grid along profiles spaced approximately 50 cm apart, taking into account areas where measurements

could not be performed due to dense vegetation or the presence of trees. Data processing was carried out using standard procedures. Distorted or saturated readings, as well as isolated point anomalies (so-called "spikes"), were excluded from further processing. Such point anomalies were defined as values exceeding 1000 nT/m relative to both neighboring measurement points.

Subsequently, the cleaned dataset was interpolated using kriging, with simultaneous exclusion of areas lacking data coverage. In the visualizations, zones of positive vertical magnetic gradient are marked in orange, while negative values are shown in blue.

The vertical magnetic gradient is calculated as the difference between the reading from the lower sensor and that from the upper sensor. In this study, the vertical spacing between the sensors was set to 1 meter, as the focus was on detecting near-surface features. A positive magnetic response is expected directly above zones containing ferromagnetic materials, while a negative response typically appears at some distance from such sources. Due to the proximity of metallic elements, such as the aforementioned fence, extreme values observed on the gradient maps should be attributed primarily to these surface or near-surface interferences.

Electromagnetic conductivity method (FDEM)

The survey was conducted using a quasi-regular measurement grid, including areas where data acquisition was not possible due to dense undergrowth or the presence of trees. Data processing followed standard procedures. Distorted or saturated measurements, as well as isolated point anomalies (commonly referred to as "spikes"), were excluded from further analysis.

A one-dimensional (1D) inversion of the resistivity data was carried out, whereby for each field curve a model curve was calculated to minimize the misfit. The maximum acceptable error was set at 5%. Each measurement point was treated as an individual sounding, and the 1D interpretation was performed separately for every location.

The resulting data were interpolated using kriging, with areas lacking data coverage excluded from the final interpolation. In the visualizations, zones of high resistivity are shown in red, while zones of low resistivity are marked in blue.

Results of the geophysical research

This chapter presents the results of geophysical measurements conducted across five designated survey polygons. Each area is analyzed individually, following a predetermined sequence. The presentation begins with maps obtained from magnetometric surveys. For each area, a pair of maps is shown: on the left, the distribution of the total magnetic field visualized on a shaded relief map, and on the right, the map of the vertical magnetic gradient. To eliminate the influence of global field variations and to focus solely on residual anomalies, the total magnetic field data were normalized in advance. The normalization process was based on reference data obtained from the Central Geophysical Observatory in Belsk, made available through the *Intermagnet* network.

Subsequently, for each area, an analogous set of maps is provided, indicating potential structures that may correspond to burial sites. These maps aim to visualize possible interpretations of the geophysical anomalies in the context of the targeted archaeological features.

Following the same structure, results obtained using the electromagnetic conductivity method are presented. For each analysed area, a series of six maps illustrates the distribution of electrical conductivity (the inverse of resistivity) at selected investigation depths: 0.25 m, 0.5 m, 0.8 m, 1.1 m, 1.6 m, and 2.3 m. Potential locations of subsurface features interpreted as burial-related structures are then marked on each of these maps. This presentation format allows for a comparative analysis of results obtained using two independent methods and facilitates the assessment of spatial consistency in the interpretation.

Area 1

Figures 16 and 17 present the results of magnetometric measurements conducted in the area designated as Polygon 1. On the map of the total magnetic field, a clearly defined, quasi-rectangular anomaly is visible. In its central part, this feature coincides with a characteristic transition zone between a positive and a negative maximum on the map of the vertical magnetic gradient. This configuration may indicate the presence of a disturbed subsurface structure - most likely a linear feature such as a trench - initially interpreted as a potential mass grave. Notably, the orientation of the anomaly is perpendicular to the direction of the survey profiles,

which reduces the likelihood of the so-called "striping effect" caused by acquisition directionality. In other parts of the polygon, numerous point anomalies are observed, though their origins remain ambiguous. These suggest a high level of signal disturbance and noise within the surveyed area.

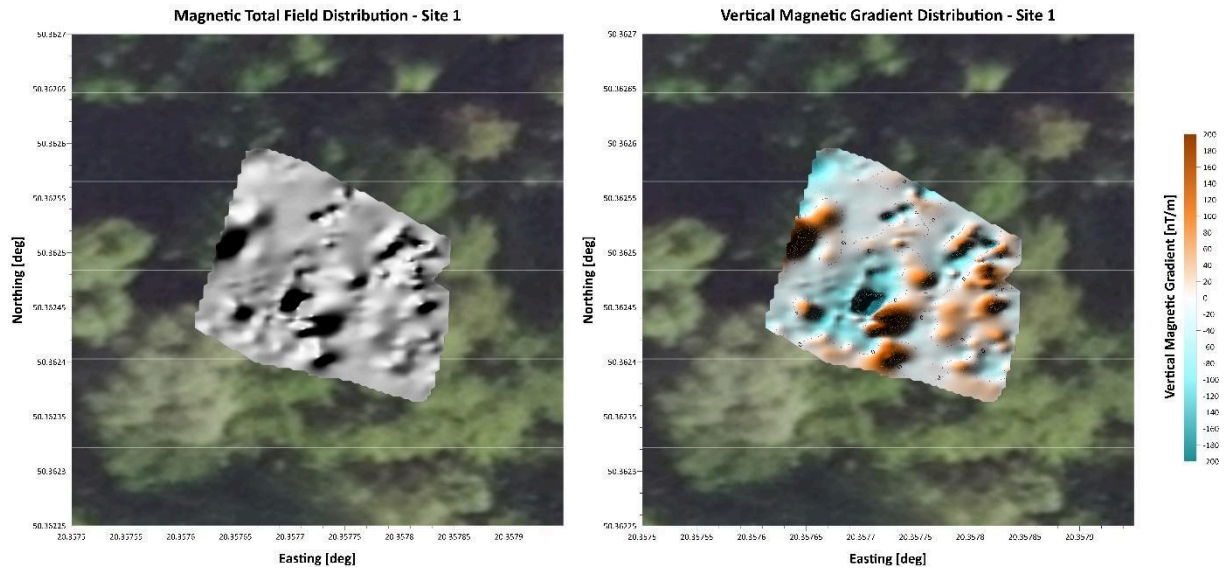


Fig. 16. Distribution of the total magnetic field (left) and the vertical magnetic gradient (right) within the boundaries of survey area no. 1.

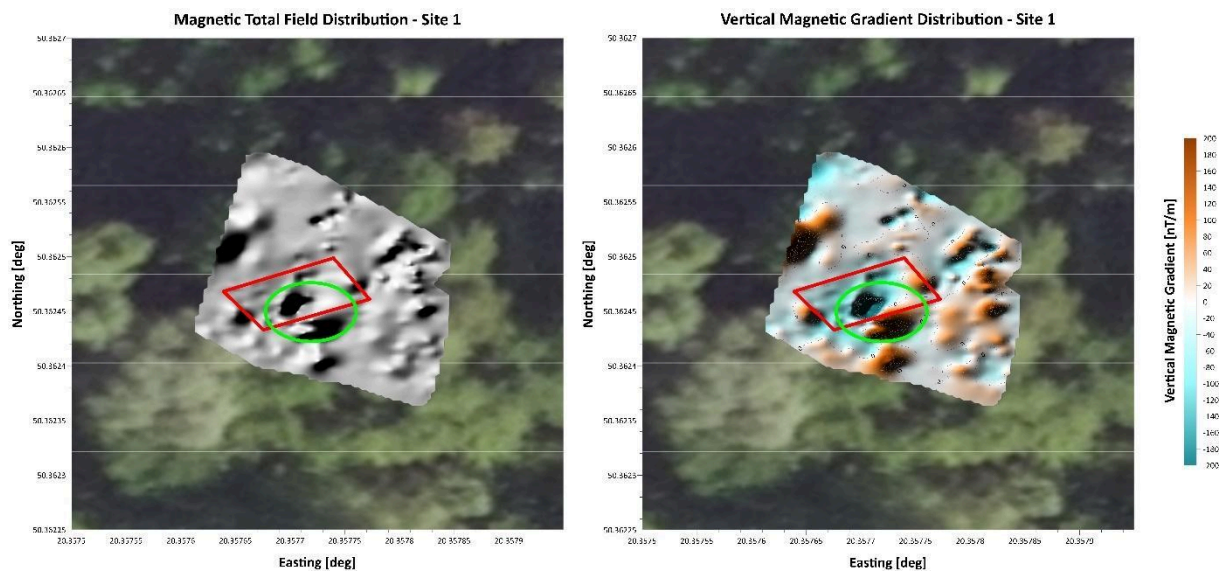


Fig. 17. Distribution of the total magnetic field (left) and the vertical magnetic gradient (right) within the boundaries of survey area no. 1, with the magnetic anomaly interpreted from magnetometric data marked in red and the anomaly interpreted from conductivity data marked in green.

Figures 18 and 19 present the distribution of electrical resistivity for Polygon 1, obtained using the electromagnetic conductivity method. In the area corresponding to the previously identified magnetic anomaly, a dominant resistivity structure is clearly visible. This feature is characterized by low resistivity values in the near-surface layers—down to approximately 1 meter in depth -followed by a transition into a zone of elevated resistivity. This pattern stands in clear contrast to the surrounding substrate, where resistivity variation with depth is significantly less pronounced.

The interpretation of this anomaly may suggest the presence of an anthropogenic feature -potentially a mass grave - in which human remains are located below the 1-meter depth, with the overlying space filled by highly conductive material, such as locally occurring clays or fluvial silts. This type of resistivity contrast may result from both the physical properties of the backfill material and structural disturbances within the natural lithological setting.

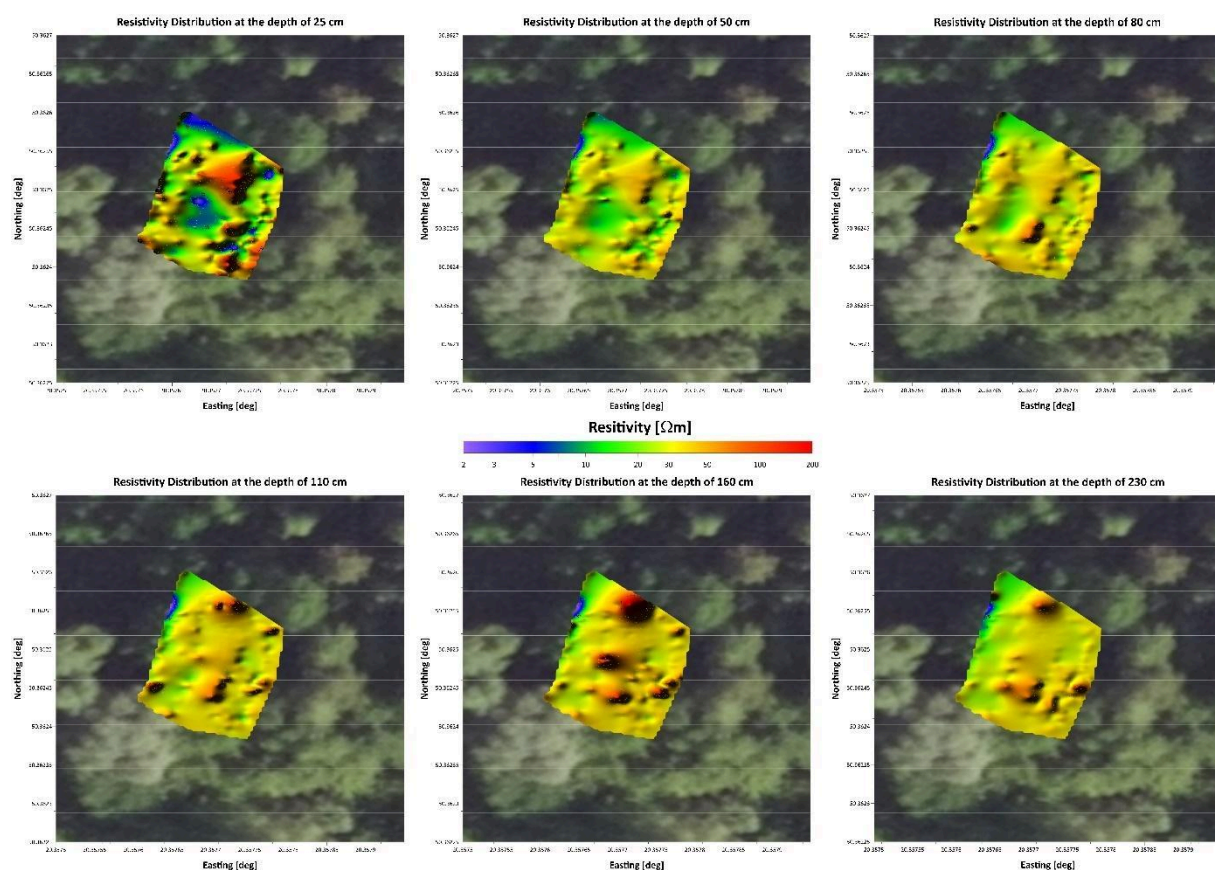


Fig. 18. Distribution of subsurface electrical resistivity at depths of 0.25, 0.5, 0.8, 1.1, 1.6, and 2.3 m within the boundaries of survey area no. 1.

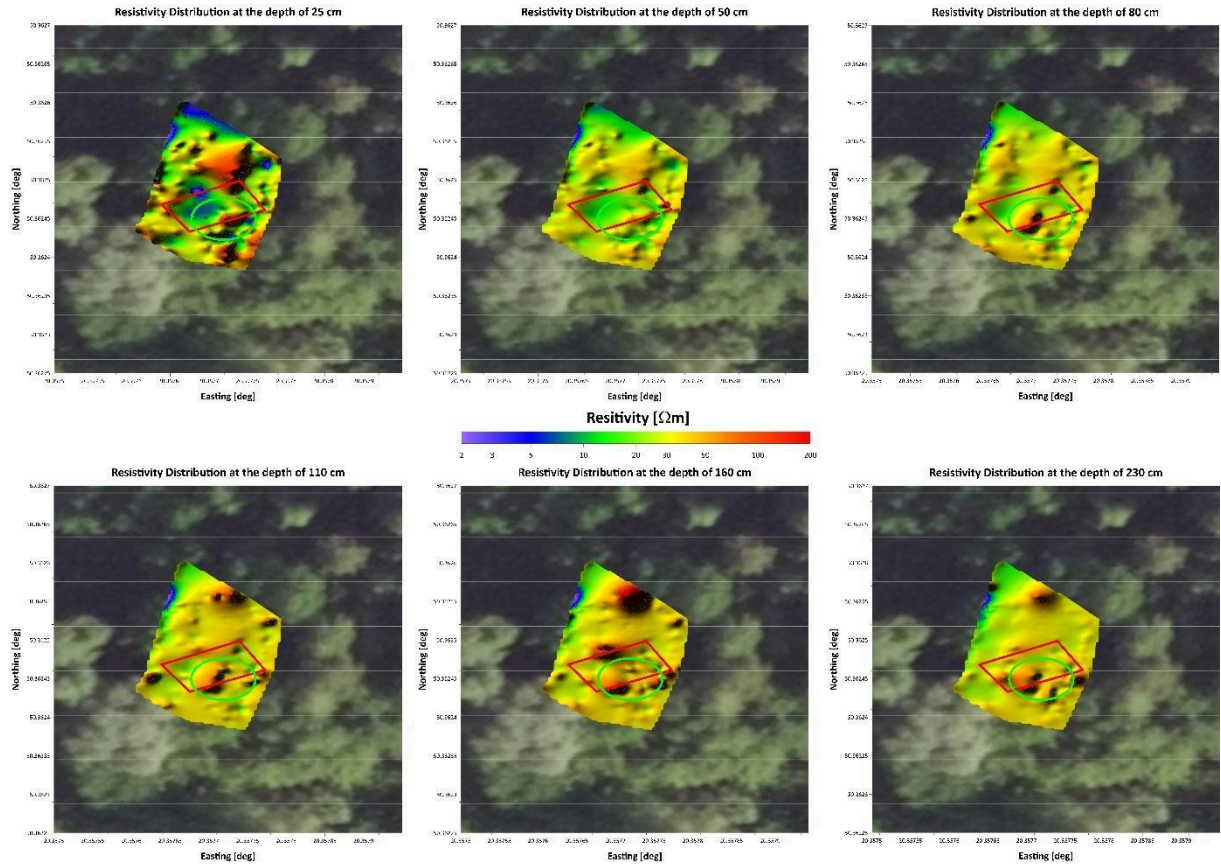


Fig. 19. Distribution of subsurface electrical resistivity at depths of 0.25, 0.5, 0.8, 1.1, 1.6, and 2.3 m within the boundaries of survey area no. 1, with the magnetic anomaly interpreted from magnetometric data marked in red and the anomaly interpreted from conductivity data marked in green.

Area 2

Figures 20 and 21 present the results of magnetometric measurements conducted within the area designated as Polygon 2. In the northern part of the surveyed area, an anomalous structure is visible, consisting of two closely spaced maxima of the vertical magnetic gradient, separated by a local minimum. This pattern is also reflected on the map of the total magnetic field; however, the structure as a whole appears less distinct and more difficult to interpret compared to the anomaly observed in Polygon 1.

Additionally, a strong magnetic effect is visible in the eastern part of the polygon, which can be clearly attributed to the presence of a metal fence surrounding the nearby monument, located in close proximity to the measurement area. Compared to

Polygon 1, the number of point anomalies interfering with interpretation is lower, resulting in a slightly higher overall clarity of the data. It is worth noting that Polygons 1 and 2 are directly adjacent to each other, allowing for their spatial correlation in the subsequent analysis.

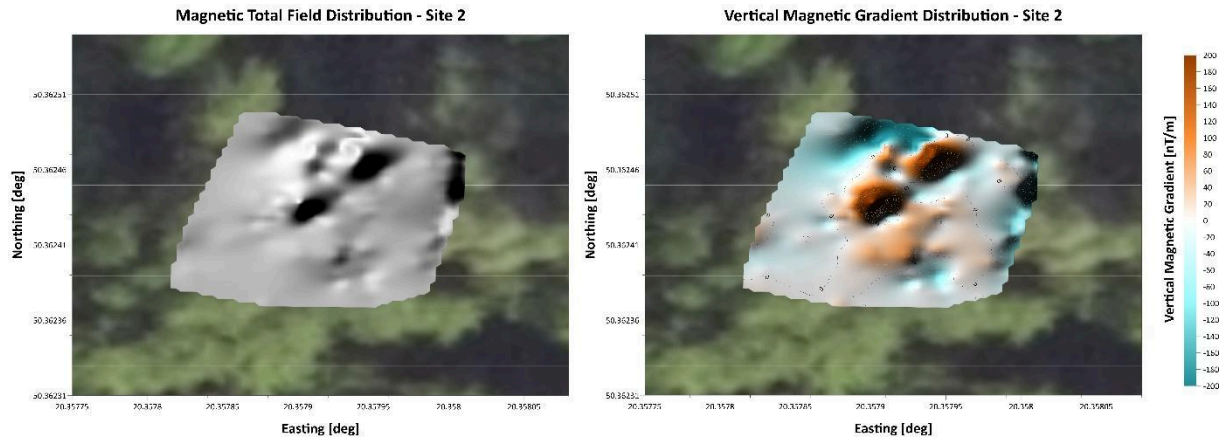


Fig. 20. Distribution of the total magnetic field (left) and the vertical magnetic gradient (right) within the boundaries of survey area no. 2.

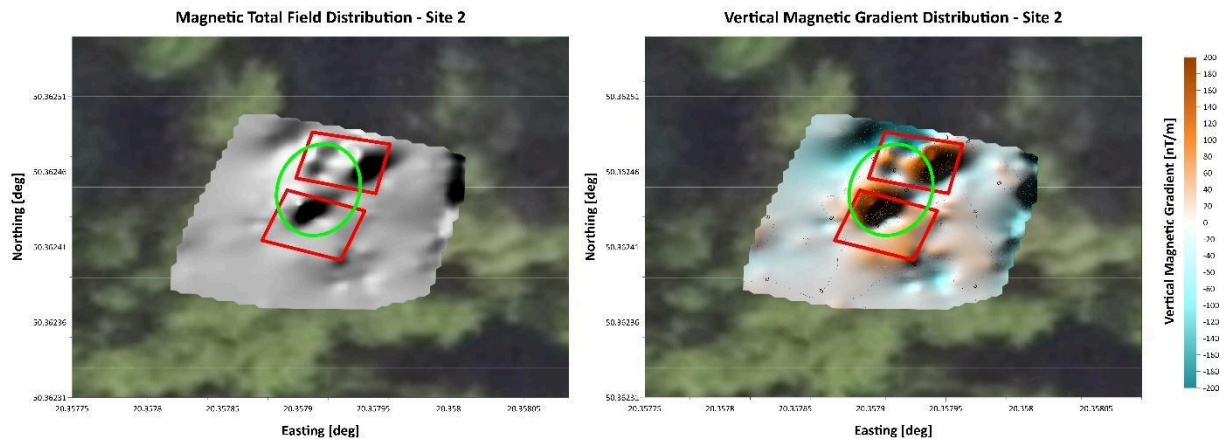


Fig. 21. Distribution of the total magnetic field (left) and the vertical magnetic gradient (right) within the boundaries of survey area no. 2, with the magnetic anomaly interpreted from magnetometric data marked in red and the anomaly interpreted from conductivity data marked in green.

A different picture compared to the magnetic data is presented by the distribution of electrical resistivity, as shown in figures 22 and 23. In this dataset, a clear linear anomaly is visible in the eastern part of the polygon, which can be confidently associated with the course of the metal fence—previously identified as a source of interference in the magnetometric measurements.

A pronounced division of the surveyed area is especially evident in the shallower depth intervals: the southern part of the polygon is characterized by higher resistivity values, while the northern part shows lower values. This contrast gradually diminishes with increasing depth.

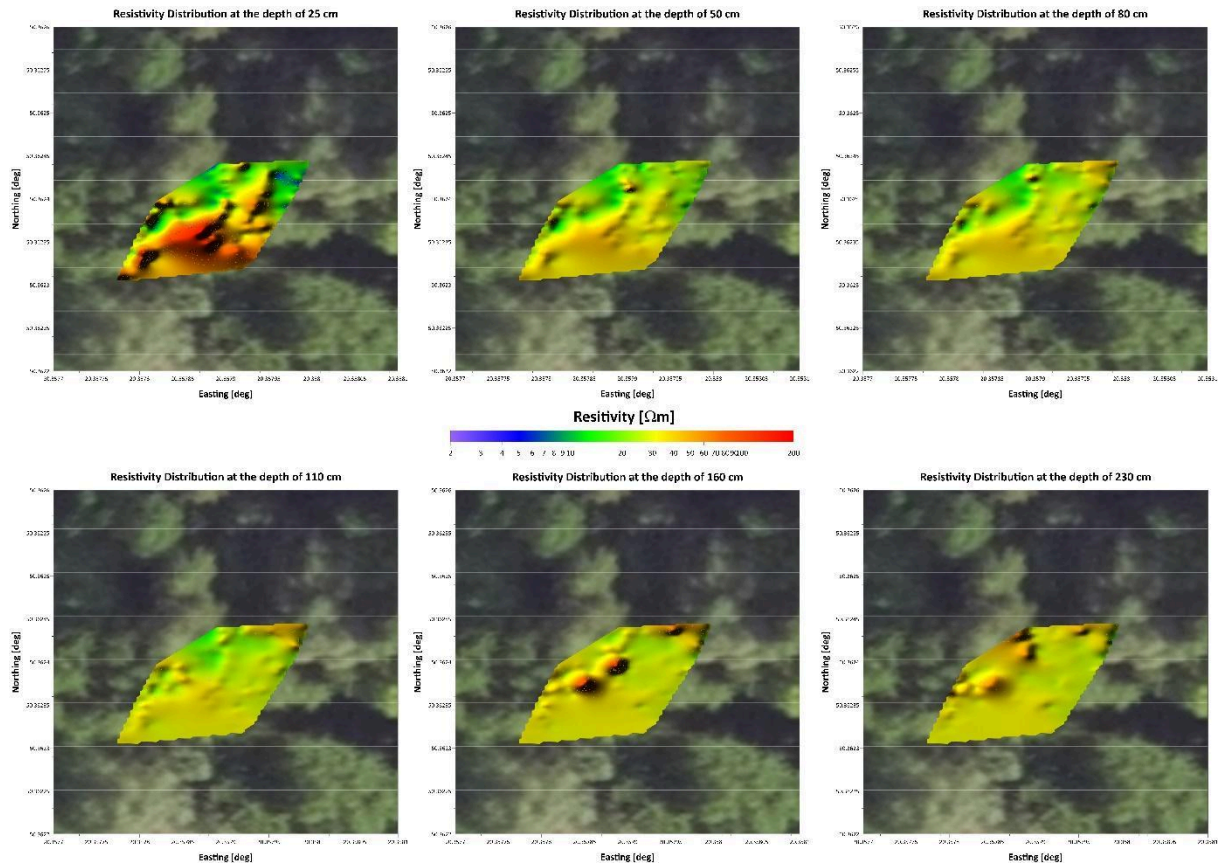


Fig. 22. Distribution of subsurface electrical resistivity at depths of 0.25, 0.5, 0.8, 1.1, 1.6, and 2.3 m within the boundaries of survey area no. 2.

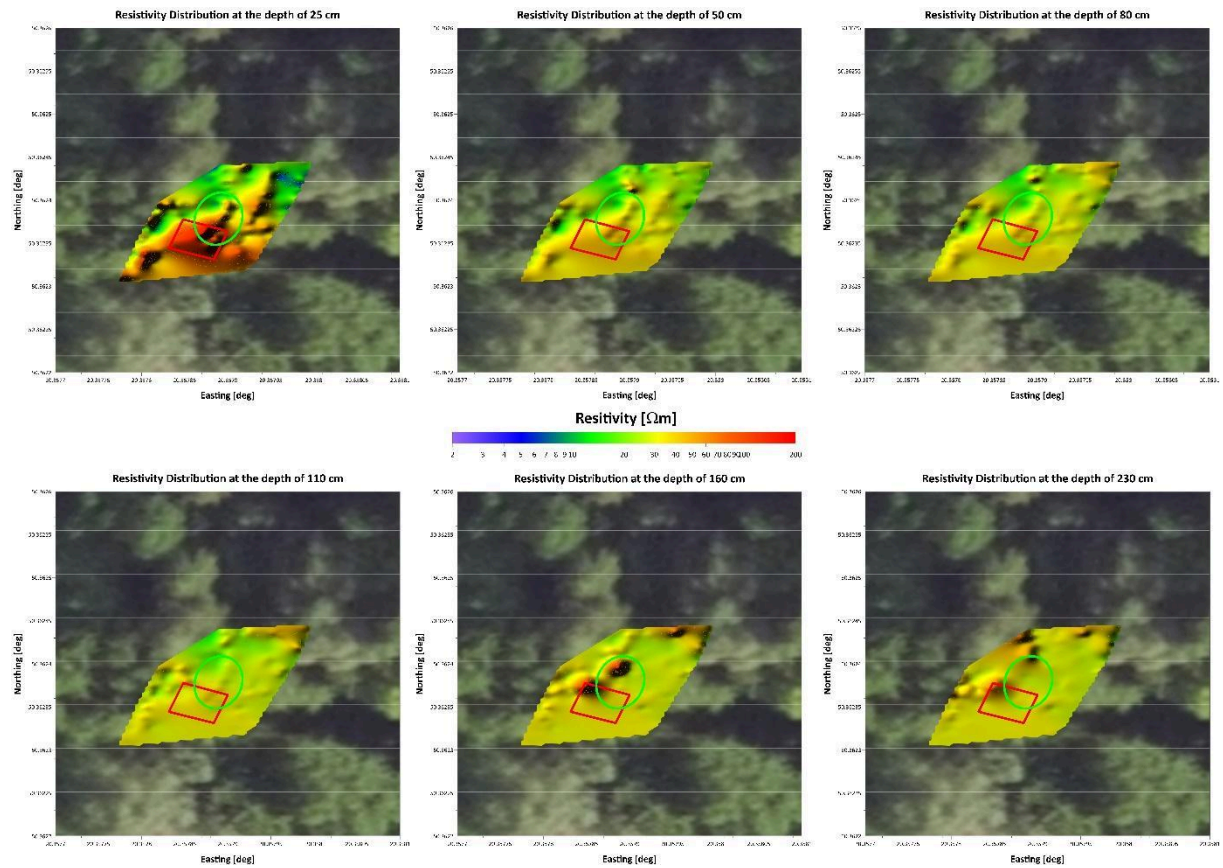


Fig. 23. Distribution of subsurface electrical resistivity at depths of 0.25, 0.5, 0.8, 1.1, 1.6, and 2.3 m within the boundaries of survey area no. 2, with the magnetic anomaly interpreted from magnetometric data marked in red and the anomaly interpreted from conductivity data marked in green.

Area 3

The results of magnetometric measurements for Polygon 3, presented in Figures 24 and 25, appear to be relatively straightforward in terms of interpretation. The dominant anomaly is located in the western part of the area, where a strong magnetic response is observed - clearly associated with the presence of a metal fence surrounding the monument. In the central part of the polygon, a cluster of positive point anomalies is visible on the vertical magnetic gradient map, partially reflected in the irregular pattern of the total magnetic field distribution.

This structure has been marked with a maroon dashed circle, indicating an area of ambiguous interpretative character - there is a lack of clear evidence for determining its origin, although its potentially anthropogenic nature cannot be excluded.

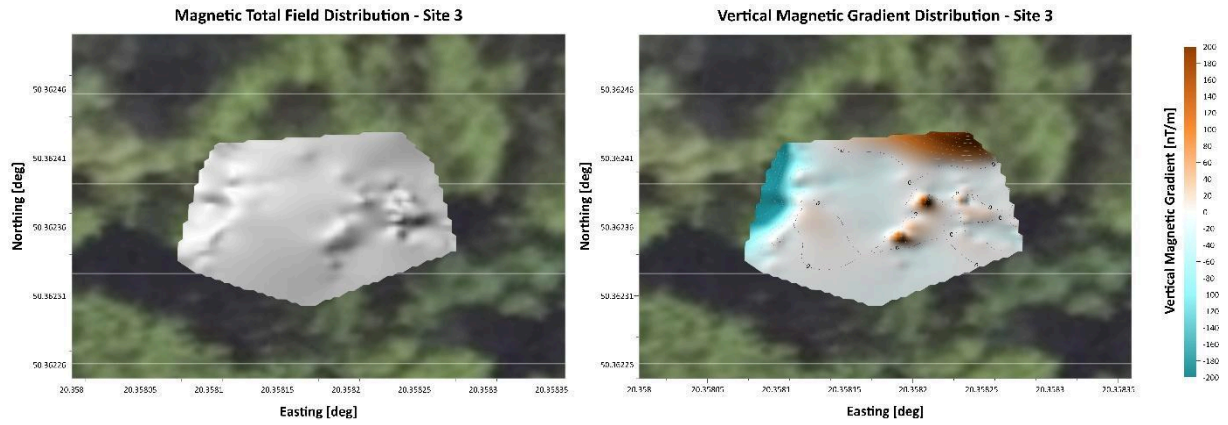


Fig. 24. Distribution of the total magnetic field (left) and the vertical magnetic gradient (right) within the boundaries of survey area no. 3.

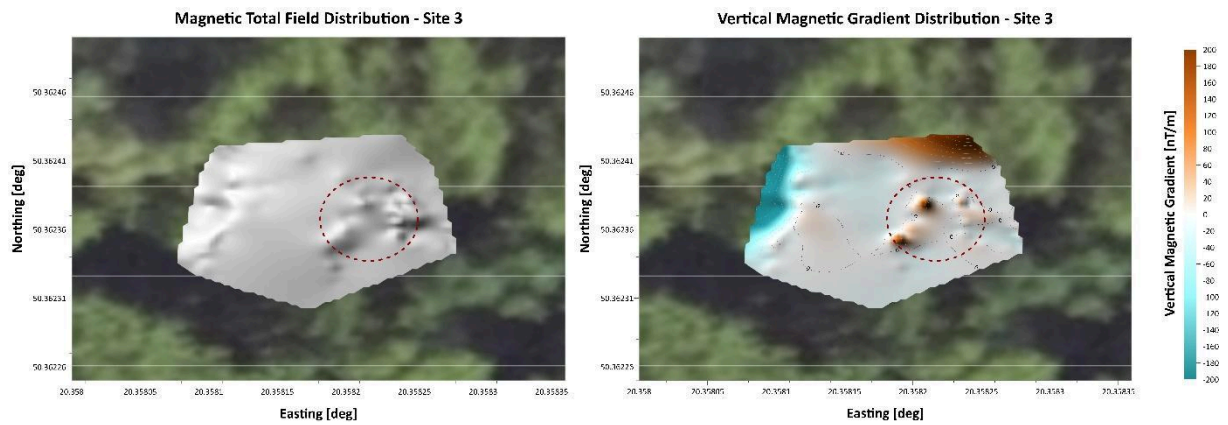


Fig. 25. Distribution of the total magnetic field (left) and the vertical magnetic gradient (right) within the boundaries of survey area no. 3, with the magnetic anomalies marked in dashed red lines.

Figures 26 and 27 show the distribution of electrical resistivity for Polygon 3. Similar to the magnetometric data, the dominant interpretative feature is a strong anomaly located in the western part of the area, resulting from the influence of the metal fence surrounding the monument. Notably, the near-surface resistivity values are significantly higher than those observed in the previously analysed polygons, despite their close spatial proximity. This may indicate local variations in lithological properties or moisture conditions.

In the eastern part of the polygon, a cluster of point anomalies -local resistivity maxima - can be observed. The origin of these anomalies remains unclear. While their spatial distribution suggests a certain degree of coherence, there is no clear

correlation with the magnetometric data or the archaeological context, making their interpretation ambiguous.

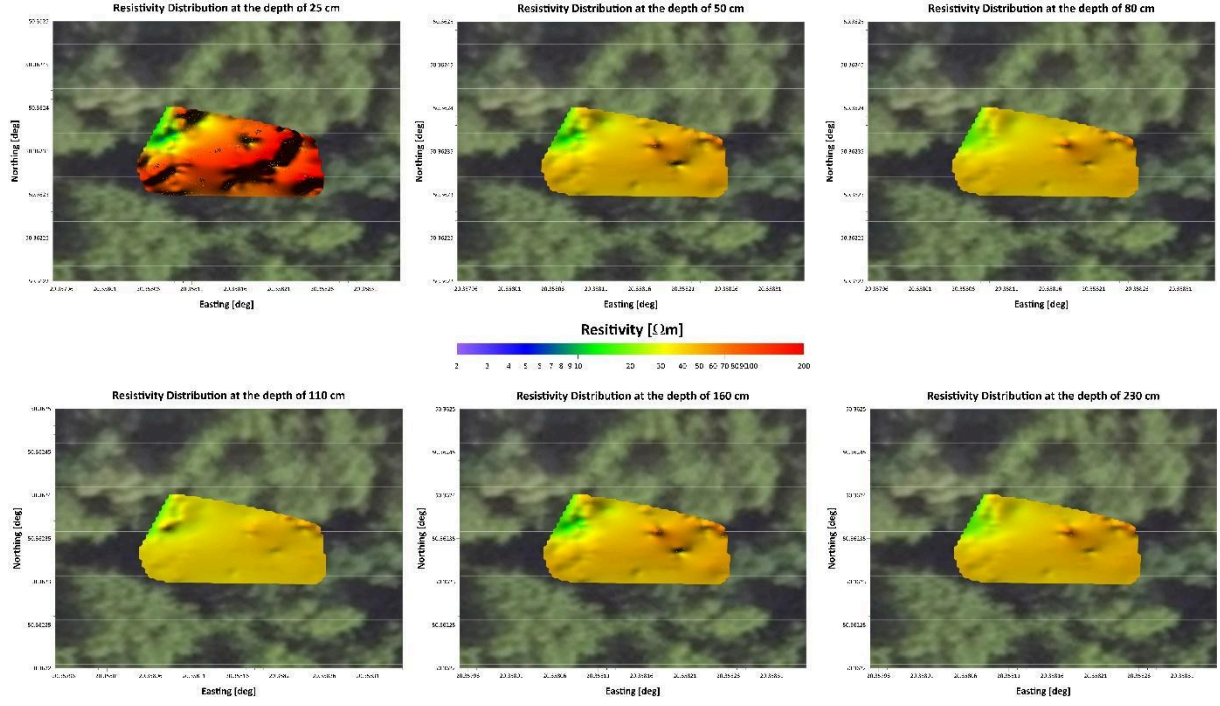


Fig. 26. Distribution of subsurface electrical resistivity at depths of 0.25, 0.5, 0.8, 1.1, 1.6, and 2.3 m within the boundaries of survey area no. 3.

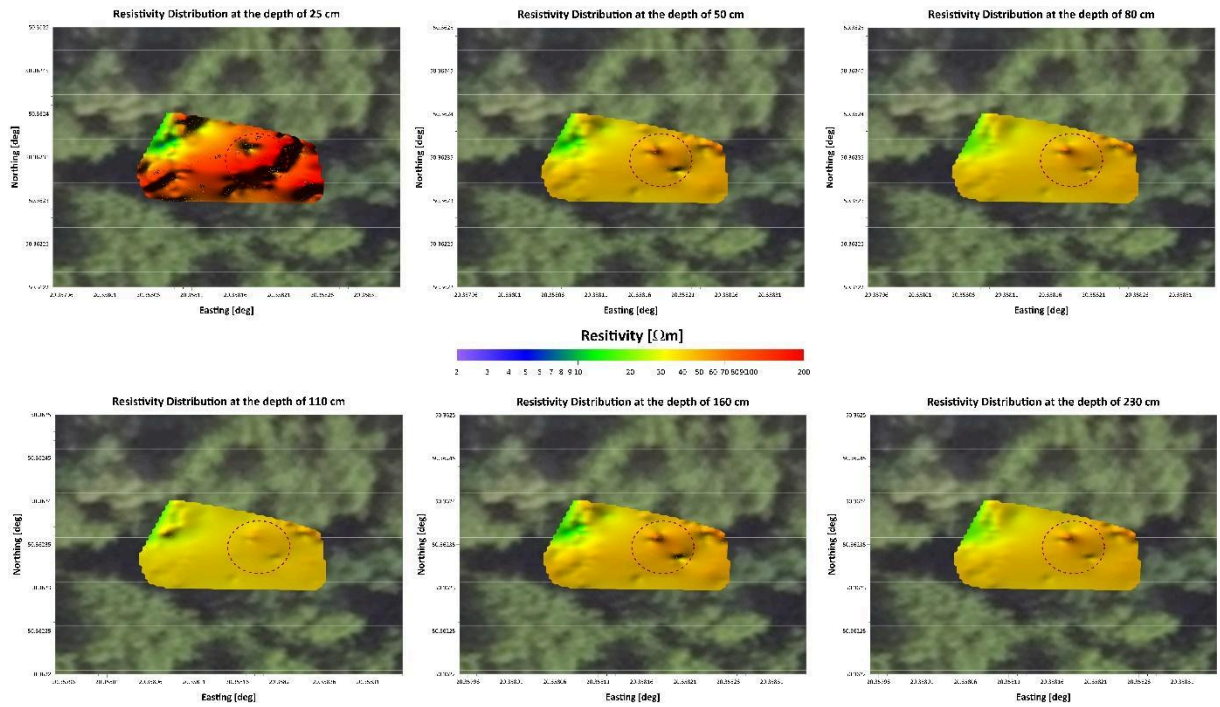


Fig. 27. Distribution of subsurface electrical resistivity at depths of 0.25, 0.5, 0.8,

1.1, 1.6, and 2.3 m within the boundaries of survey area no. 3, with the magnetic anomalies marked in dashed red lines.

Area 4

The results of magnetometric measurements for Polygon 4 are presented in figures 28 and 29. One of the key features distinguishing this area from the previously analyzed polygons is the noticeably weaker magnetic response. The values of the vertical magnetic gradient range from -50 to +50 nT/m, which contrasts with the broader scale of -200 to +200 nT/m used in the data visualizations for Polygons 1 - 3. This lower signal intensity results in generally weaker contrast between magnetic anomalies in this area.

In the central part of the polygon, a small cluster of local maxima and minima in the magnetic gradient was recorded, which partially corresponds with linear structures visible on the total magnetic field map. However, this correlation is not clear-cut, and the interpretation of these features is far less distinct than in the case of, for example, Polygon 1. A potential area indicating the presence of an anthropogenic structure has been marked with a maroon dashed rectangle and circle, identifying a zone that requires further verification.

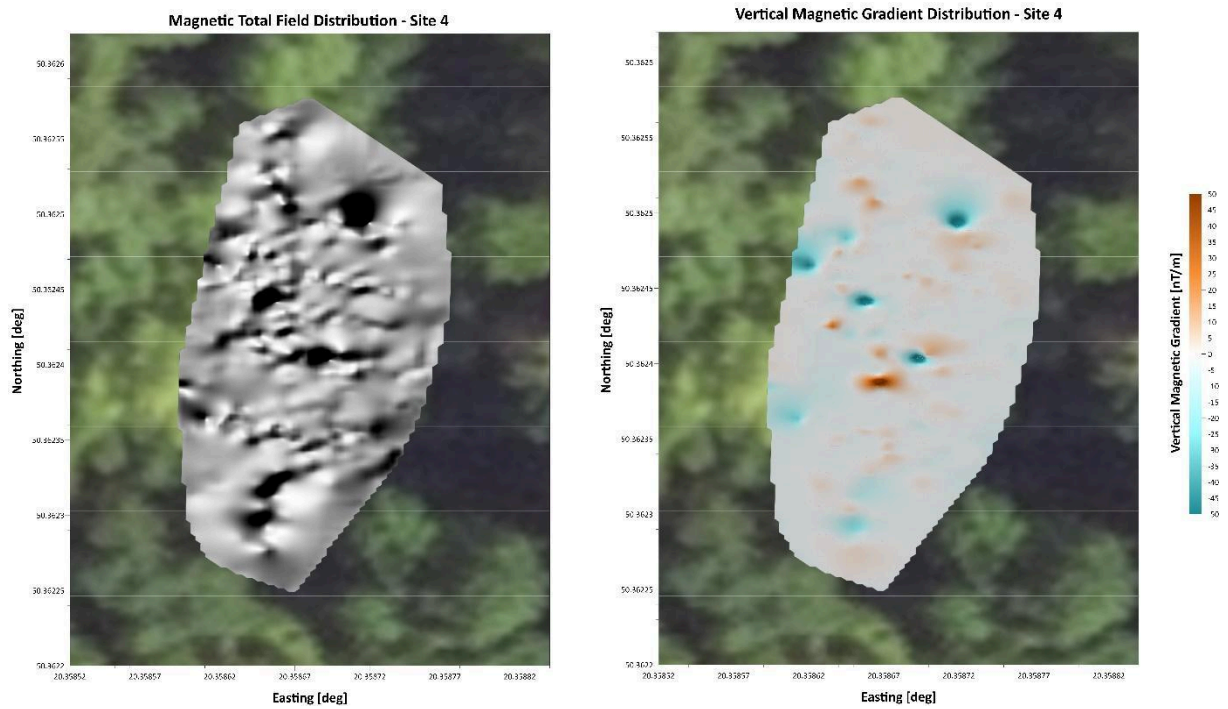


Fig. 28. Distribution of the total magnetic field (left) and the vertical magnetic gradient (right) within the boundaries of survey area no. 4.

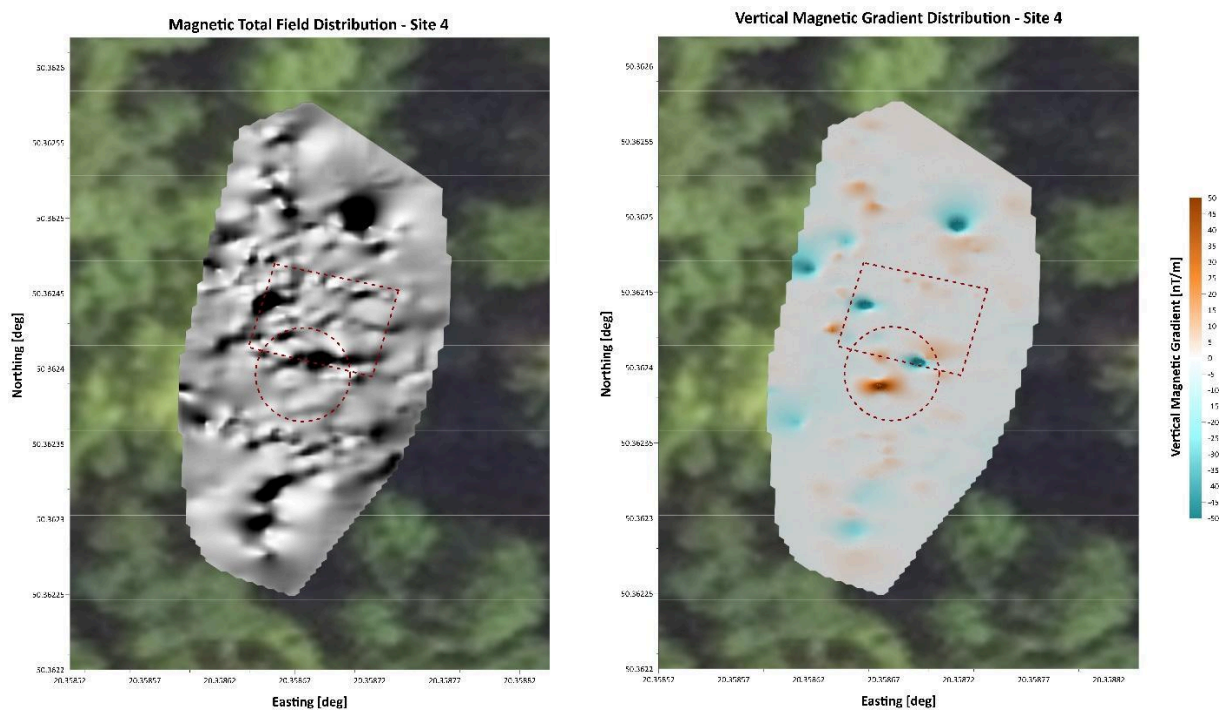


Fig. 29. Distribution of the total magnetic field (left) and the vertical magnetic gradient (right) within the boundaries of survey area no. 4, with the magnetic anomalies marked in dashed red lines.

In the case of Polygon 4, the most promising results were obtained using the electromagnetic conductivity method. These results are presented in figures 30 and 31. Excluding the near-surface layer - which exhibited extremely high resistivity values, most likely due to the drying of loess deposits - deeper layers revealed a distinct linear pattern of resistivity variation, oriented transversely to the axis of the ravine. The northern and southern parts of the area are dominated by high-resistivity structures, while in the central part, a zone of lower electrical resistivity emerges, morphologically resembling a channel or trench.

Within this central zone, at depths of up to approximately 1 meter, a structure with elevated resistivity is observed - comparable to that of the surrounding layers. Below this level, resistivity decreases again, approaching the values of the geological background. This phenomenon may indicate the presence of a filled void (e.g., a cavity or trench) that was backfilled with material originating from the surrounding area - a scenario consistent with anthropogenic infilling. Notably, the spatial position of this structure corresponds with the previously described magnetic anomaly, reinforcing the hypothesis of a potential archaeological feature. At the same time, due to the specific topography and genesis of the ravine, the influence of natural denudation processes on the observed resistivity pattern cannot be ruled out.

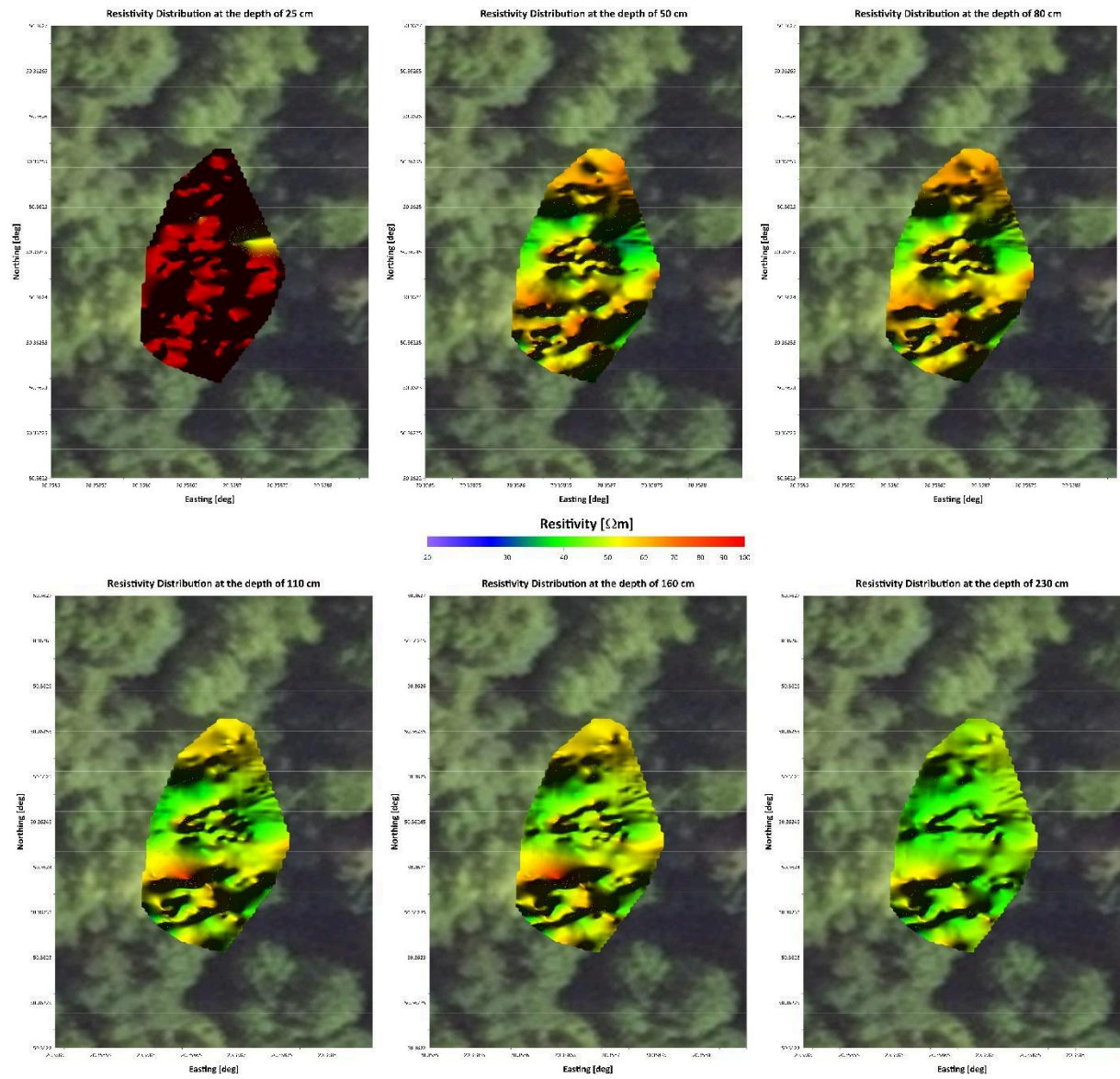


Fig. 30. Distribution of subsurface electrical resistivity at depths of 0.25, 0.5, 0.8, 1.1, 1.6, and 2.3 m within the boundaries of survey area no. 4.

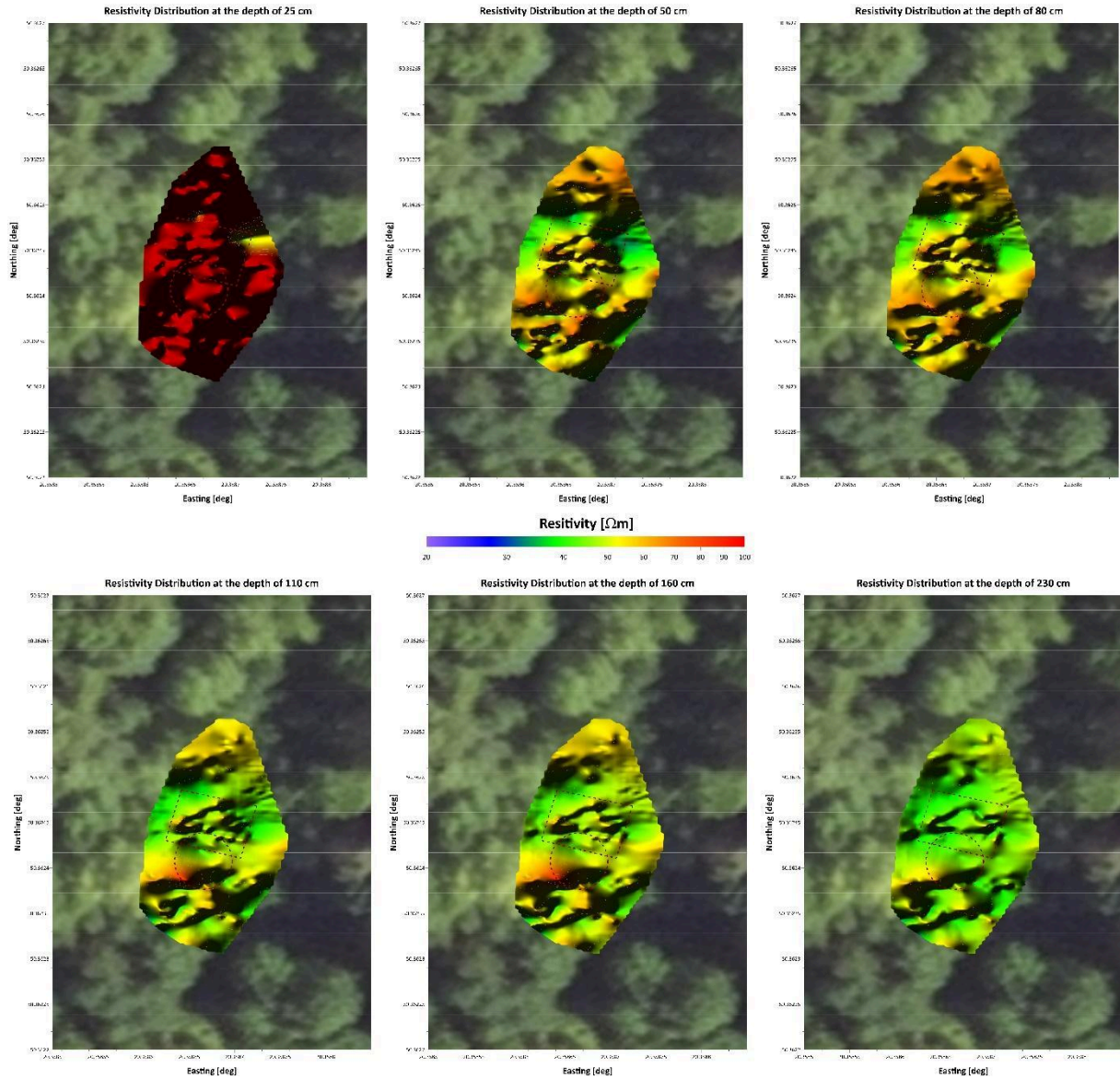


Fig. 31. Distribution of subsurface electrical resistivity at depths of 0.25, 0.5, 0.8, 1.1, 1.6, and 2.3 m within the boundaries of survey area no. 4, with the magnetic anomalies marked in dashed red lines.

Area 5

Polygon 5 was located near a forest road, specifically at the junction of two forest paths, which gave it an unusual triangular shape. The results of the magnetometric measurements are presented in figures 32 and 33. Compared to Polygon 4, the recorded anomalies are stronger; however, it should be noted that this area was heavily contaminated with surface debris - numerous scattered metal objects were present, including fragments of wire, pots, bottles, and other items capable of generating magnetic interference.

Along the northern edge of the polygon, adjacent to the road, a cluster of point-like maxima and minima in the magnetic gradient is visible. However, interpreting the origin of these anomalies is difficult. The area is also characterized by an irregular and ambiguous pattern in the distribution of the total magnetic field. Due to the presence of numerous disturbances and the overall uncertainty of the signal, the results from this polygon should be treated with caution - as supplementary data requiring validation through additional methods.

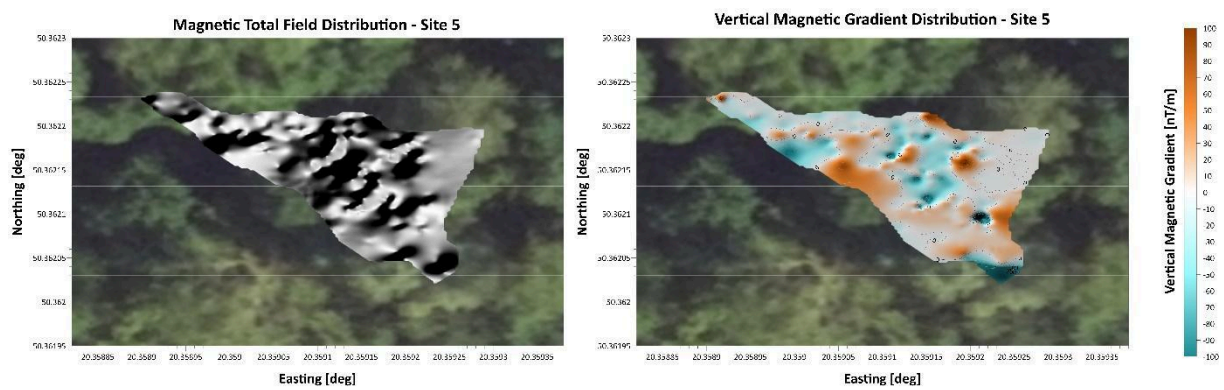


Fig. 32. Distribution of the total magnetic field (left) and the vertical magnetic gradient (right) within the boundaries of survey area no. 5.

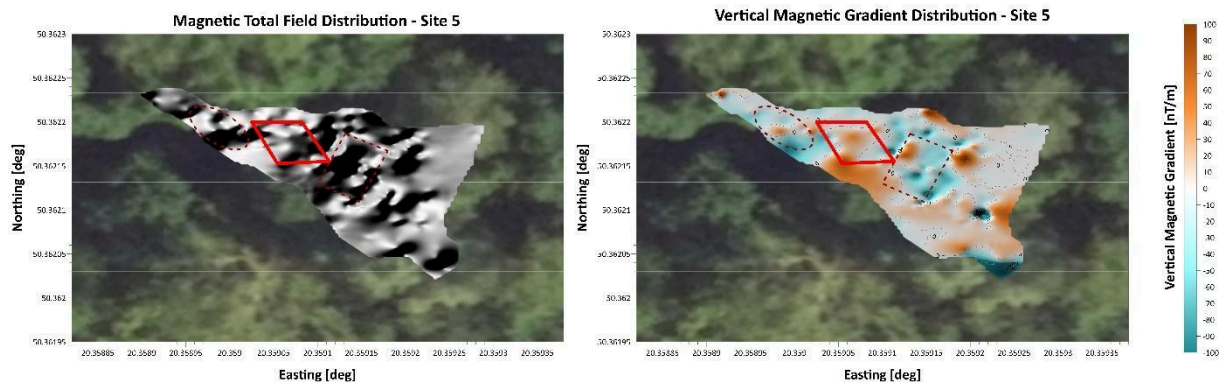


Fig. 33. Distribution of the total magnetic field (left) and the vertical magnetic gradient (right) within the boundaries of survey area no. 5, with the magnetic anomalies marked in dashed red lines.

The results of conductivity measurements for Polygon 5 are presented in figures 34 and 35. The most prominent feature in the resistivity data is a high-resistivity zone located in the northeastern part of the polygon, interpreted as an artificially formed earthen mound situated adjacent to the road. This structure is particularly well

defined at depths ranging from approximately 0.8 to 1.6 meters below the ground surface, but it is not clearly visible in the deepest measurement range.

In other parts of the area, local point anomalies with low resistivity values were recorded at depths of up to about 0.5 meters. Some of these anomalies show partial correlation with the magnetometric data; however, their scattered distribution and shallow depth suggest they are likely associated with small metallic objects in the near-surface layer - such as the previously identified wires, fragments of cookware, or bottles. The only anomaly for which a clear and consistent correlation between resistivity and magnetometric data exists is the aforementioned mound, whose presence is likely linked to anthropogenic surface modification.

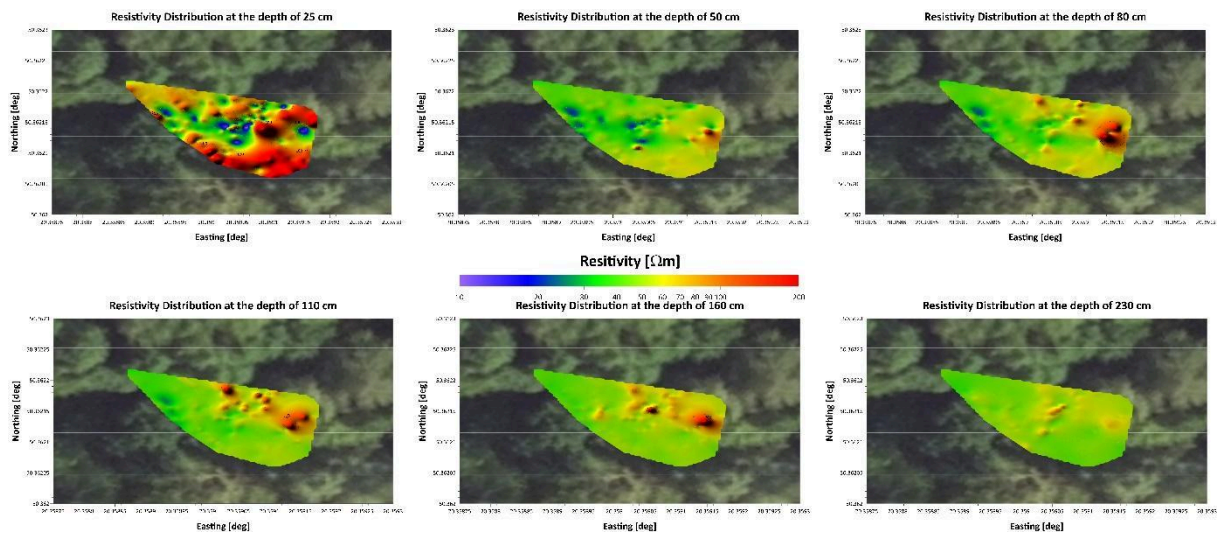


Fig. 34. Distribution of subsurface electrical resistivity at depths of 0.25, 0.5, 0.8, 1.1, 1.6, and 2.3 m within the boundaries of survey area no. 5.

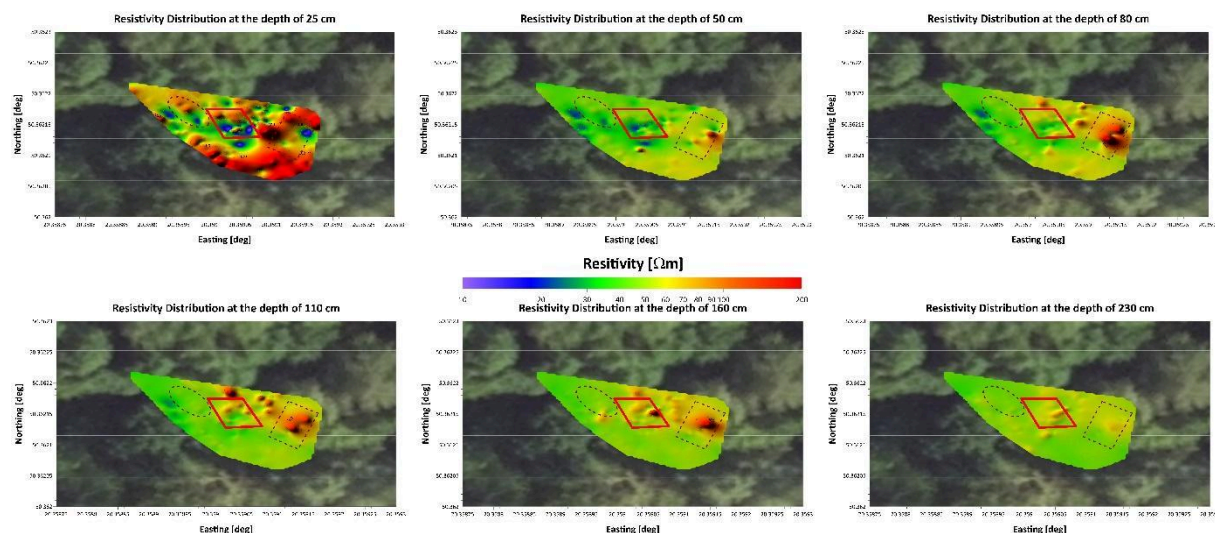


Fig. 35. Distribution of subsurface electrical resistivity at depths of 0.25, 0.5, 0.8, 1.1, 1.6, and 2.3 m within the boundaries of survey area no. 5, with the magnetic anomalies marked in dashed red lines.

Summary of results of the geophysical research

The geophysical surveys conducted using gradient magnetometry and electromagnetic conductivity methods enabled the identification of several structures of potential archaeological significance, as well as the detection of features and phenomena associated with signal interference. The character and intensity of the recorded anomalies varied significantly between the analyzed polygons, which can be attributed both to local geological and geomorphological conditions and to the presence of interfering elements such as metal fences or scattered surface debris.

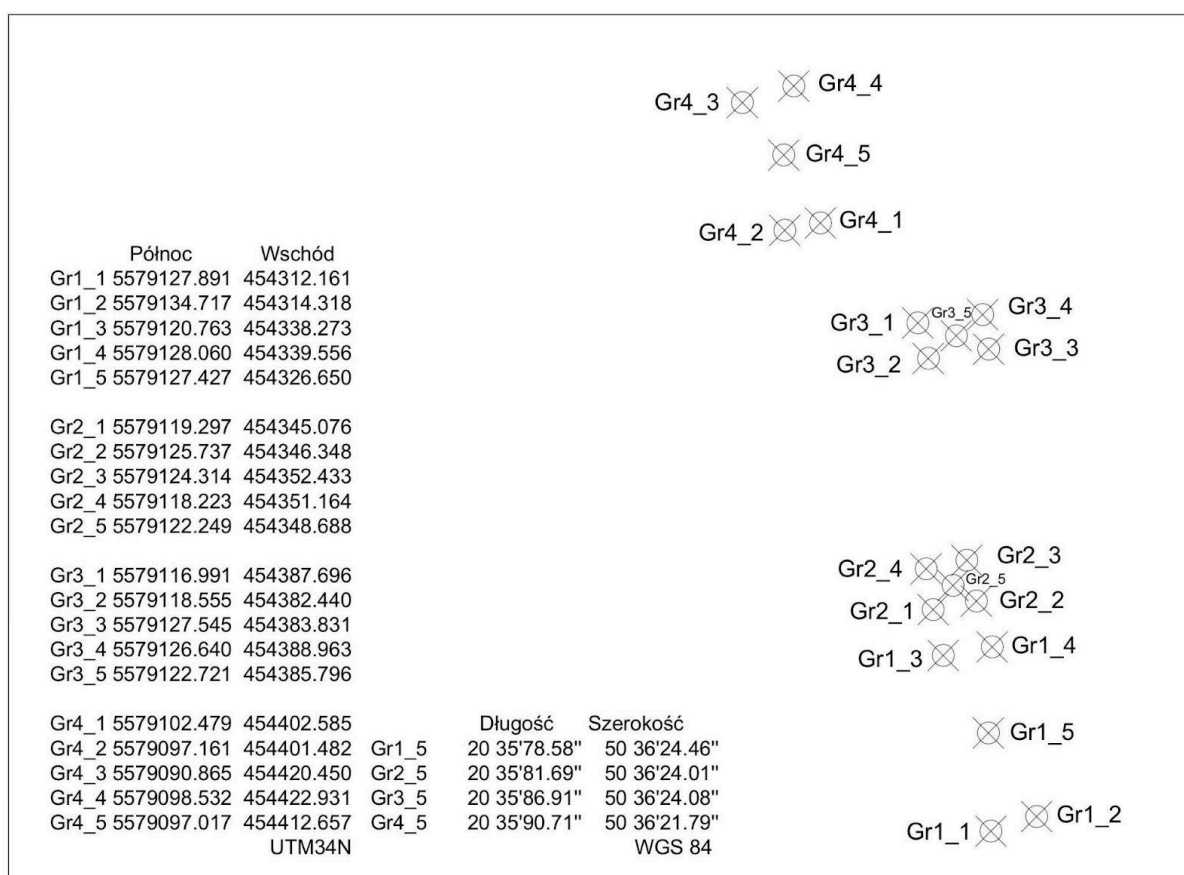
The most distinct and spatially coherent anomalies were recorded in Polygons 1 and 4, where data from both methods suggest the presence of structures with a potentially anthropogenic origin. In particular, for Polygon 1, the correlation between magnetic and resistivity results allows for the preliminary identification of an anomaly that may correspond to a mass grave. Similarly, in Polygon 4—despite the weaker magnetic effects—the conductivity data revealed the presence of features that may be relevant from an archaeological prospection perspective.

Polygons 2 and 3 were affected by interference related to the proximity of fencing and varying degrees of data noise; however, localized correlations between the two methods were still observed. In the case of Polygon 5, due to extensive surface litter and an unusual topographic configuration, data interpretation proved most challenging. Only within the area of an earthen mound in the northeastern part of the polygon was a consistent conductivity anomaly recorded, partially confirmed by magnetometric data.

Conclusions

In the first half of 2025, the Zapomniane Foundation conducted comprehensive non-invasive research on the grounds of the former Jewish cemetery in Działoszyce and its surroundings. The aim was to locate execution and burial sites of victims of mass crimes committed by the Germans on September 2–3, 1942, during which approximately 1,500–1,600 people of Jewish origin were murdered. The research was conducted in accordance with Halachic principles and the guidelines of the Rabbinical Commission for Jewish Cemeteries. As a result of the work, five research areas were identified and marked on the map as follows:

- GR1 and GR2 – covering areas 1, 2, and 3,
- GR3 – area 4,
- GR4 – area 5.



Evaluation of Research Results

Areas 1, 2, and 3 (GR1 and GR2)

The results in these locations revealed strong and unambiguous geophysical anomalies, confirmed by at least two methods (magnetometry and conductivity testing), and in the case of area 2, also by ground-penetrating radar (GPR).

- Area 1 – A linear anomaly measuring approximately 9 m x 2 m was identified, with characteristics consistent with a mass grave.
- Area 2 – An anomaly was confirmed in the form of two adjacent zones, measuring approximately 6–7 m x 2.5 m, also interpreted as a burial site.
- Area 3 – The results are less clear but still suggest the presence of possible anthropogenic (man-made) structures.

The consistency of the results with eyewitness accounts, 1960s documentation, and the site's topography indicates that at least two locations can be identified with high

probability as mass war graves from September 1942 and meet the criteria for inclusion in the register of war graves.

Areas 4 and 5 (GR3 and GR4)

The research results in these locations are inconclusive and do not allow for definitive interpretation.

- Area 4 – This is a loess ravine area, which proved very difficult to effectively examine using GPR and other methods.
- Area 5 – This area is heavily contaminated with secondary metal debris and has significant topographic disturbances.

Despite technical limitations, it is important to emphasize that both locations were identified by an eyewitness as potential execution and burial sites. Therefore, they should be treated as areas of particular commemorative and protective concern, even if current knowledge does not permit clear structural documentation of burials.

Conclusions and Recommendations

Areas 1, 2, and 3 meet the criteria to be recognized as mass burial sites of World War II victims and should be submitted for inclusion in the register of war graves.

Areas 4 and 5 – Despite the lack of clear findings, due to strong eyewitness testimony, it is recommended that these sites be permanently marked, secured, and commemorated.

The results of the research provide a solid foundation for further documentation, educational initiatives, and commemorative efforts in the Działoszyce area.